

A MICROPSORIDIAN PARASITE INFECTS RIBBON WORMS OF THE GENUS

*MACULAURA* ON THE EASTERN PACIFIC COAST

by

KARA MEGAN ROBBINS

A THESIS

Presented to the Department of Biology  
and the Graduate School of the University of Oregon  
in partial fulfillment of the requirements  
for the degree of  
Master of Science

December 2018

THESIS APPROVAL PAGE

Student: Kara Megan Robbins

Title: A Microsporidian Parasite Infects Ribbon Worms of the Genus *Maculaura* on the Eastern Pacific Coast

This thesis has been accepted and approved in partial fulfillment of the requirements for the Master of Science degree in the Department of Biology by:

George von Dassow	Chairperson
Svetlana Maslakova	Member
Alan Shanks	Member
Maya Watts	Member

and

Janet Woodruff-Borden      Vice Provost and Dean of the Graduate School

Original approval signatures are on file with the University of Oregon Graduate School.

Degree awarded December 2018

© 2018 Kara Megan Robbins

## THESIS ABSTRACT

Kara Megan Robbins

Master of Science

Department of Biology

December 2018

Title: A Microsporidian Parasite Infects Ribbon Worms of the Genus *Maculaura* on the Eastern Pacific Coast

The small nemertean *Maculaura alaskensis* is used as a model for studies of pilidiophoran development. During several microinjection experiments, it became clear several batches of oocytes obtained from wild-caught females contained an intracellular pathogen. Infected oocytes have large vesicles containing dozens to hundreds of refractile oval objects. Examination of oocytes with DIC and confocal microscopy showed the spores within the vesicles were diplokaryotic and contained a coiled tube, traits that are diagnostic of the phylum Microsporidia. The Microsporidia are a group of obligate intracellular parasites that infect cells of protists and animals. No other microsporidian has ever been found infecting cells of nemerteans and the association between *M. alaskensis* and this microsporidian is, thus far, undocumented. For my thesis, I described morphological characteristics, molecular phylogeny, and geographic range of the microsporidian. Additionally, I observed parasitic influences on development of infected *M. alaskensis* and explored other potential host species.

## CURRICULUM VITAE

NAME OF AUTHOR: Kara Megan Robbins

### GRADUATE AND UNDERGRADUATE SCHOOLS ATTENDED:

University of Oregon, Eugene, OR  
University of Wyoming, Laramie, WY

### DEGREES AWARDED:

Master of Science, Biology, 2018, University of Oregon  
Bachelor of Science, Marine Biology, 2014, University of Oregon  
Bachelor of Science, Physiology, 2012, University of Wyoming

### AREAS OF SPECIAL INTEREST:

Pathology, epidemiology, and infectious disease  
Developmental and evolutionary biology  
Marine invertebrate zoology

### PROFESSIONAL EXPERIENCE:

Graduate Research Assistant, Oregon Institute of Marine Biology,  
University of Oregon, Charleston, OR, 2016 – 2018

Graduate Teaching Assistant, Oregon Institute of Marine Biology,  
University of Oregon, Charleston, OR, 2017 – 2018

Laboratory Technician II, Oregon Institute of Marine Biology,  
University of Oregon, Charleston, OR, 2014 - 2016

Student Research Assistant, Oregon Institute of Marine Biology,  
University of Oregon, Charleston, OR, 2013 – 2014

Laboratory Technician I, Wyoming State Veterinary Laboratory,  
University of Wyoming, Laramie, WY, 2012

Student Employee, Wyoming State Veterinary Laboratory,  
University of Wyoming, Laramie, WY, 2009 - 2012

#### GRANTS, AWARDS, AND HONORS:

Golden Key Honour Society, University of Wyoming Chapter, 2010-2012

President's List, University of Wyoming, 2008

Dean's List, University of Wyoming, 2008-2011

Honor's Hathaway Scholarship, University of Wyoming, 2007

President's Scholarship, University of Wyoming, 2007

Leah Joyce Memorial Scholarship, East High School, 2007

#### PRESENTATIONS:

Robbins, K., Maslakova, S., & von Dassow, G. (2018). A Microsporidian Infests Oocytes of the Ribbon Worm *Maculaura alaskensis*. *Society of Integrative and Comparative Biology*.

Robbins, K., & Watts, M. (2014). Life History and Larval Development of a Parasitic Copepod, *Ismaila belciki* on a Northeast Pacific Nudibranch *Janolus fuscus*. *Western Society of Naturalists*, 95, 133.

## ACKNOWLEDGMENTS

First, I would like to thank my advisor, Dr. George von Dassow for his ability to be unerringly perceptive, inquisitive, and patient not only in his scientific pursuits but in all aspects. His counsel and understanding have been deeply appreciated. I would also like to thank Dr. Svetlana Maslakova, Dr. Alan Shanks, and Dr. Maya Watts for agreeing to help me through this endeavor and for their input on my manuscript. I am a better scientist and communicator because of their thoughtful feedback and suggestions. Thanks to all other OIMB faculty for being impromptu mentors when I needed advice.

Additionally, I would like to thank the OIMB graduate student community for their company and friendship. Special thanks to my lab mates Nicole Moss, Nicole Nakata, Christina Ellison, Marie Hunt, Dr. Jenna Valley, Dr. Terra Hiebert, and Dr. Laurel Hiebert for assisting me in the laboratory or field, lending their samples, and allowing me to exploit their expertise. Thanks to Alexa Romersa, Zofia Knorek, Carlissa Salant, Mack Hardy and countless undergraduate and REU students for assisting with worm collection. To the OIMB staff, particularly James Johnson and the maintenance staff for fixing everything, you are awesome.

I would like to extend thanks to Dr. Poh Kheng Loi and the UO Histology Lab for training me and for embedding/sectioning many of my samples. Also to Dr. Kurt Langworthy and Dr. Josh Raznik at the CAMCOR facility for their time spent on training and troubleshooting TEM with me. To Dr. Naomi Fast of the University of British Columbia, thank you for answering my many, many questions about microsporidia. Your encouragement and advice were greatly appreciated.

I would like to thank my family and friends for their support. To my parents, for letting me explore, ask questions, and try everything. I would especially like to thank my wife, Clara, for being patient and helpful during this time of our lives. I will always appreciate you coming to spend time with me in the mud or bringing me a missed meal. Thank you for listening to me drone on, and on about the Microsporidia and for editing everything I have written over the last four years. For so many things, thank you. This was attainable because of you.



For Sierra, Korina, Eli, and Aden.

## TABLE OF CONTENTS

Chapter	Page
I. INTRODUCTION .....	1
Microsporidia .....	1
Nemertea .....	4
<i>Maculaura</i> .....	4
II. HEPATOSPORIDAE N. GEN., N. SP., A MICROSPORIDIAN PARASITE OF RIBBON WORMS IN THE GENUS <i>MACULAURA</i> ON THE EASTERN PACIFIC COAST .....	7
Introduction .....	7
Materials and Methods .....	10
Collections .....	10
Light Microscopy Analysis .....	12
DNA Extraction, PCR, and Sequencing .....	12
SSU Phylogenetic Analysis .....	13
Transmission Electron Microscopy (TEM) .....	14
Histology .....	15
Larval Development Observations .....	16
Diagnostic PCR for Detection of Hepatosporidae n. gen, n. sp. ....	16
DNA Barcoding of Infected Nemerteans .....	18
Results .....	18
Light Microscopy Observations .....	18
SSU and RPB1 Sequencing .....	19
SSU Phylogenetic Analysis .....	20

Chapter	Page
TEM .....	22
Histology.....	23
Diagnostic PCR and Nemertean Host Barcoding .....	25
Developmental Studies .....	27
Species Description for Hepatosporidae n. gen., n. sp. " <i>Oogranate sp.</i> " .....	30
Description.....	30
Diagnosis.....	30
Type Host.....	31
Type Locality .....	31
Site of Infection.....	31
Etymology.....	31
Discussion.....	31
Systematics .....	31
Host Types .....	32
Geographic Distribution.....	33
Parasite Load.....	35
Hypothesized Lifecycle .....	35
Mode of Transmission in <i>M. alaskensis</i> .....	37
Vertical Transmission.....	38
Horizontal Transmission.....	39
III. CONCLUSION.....	41
APPENDICES .....	42

Chapter	Page
A. APPENDIX A: NEMERTEAN SAMPLE COLLECTION AND EXPERIMENT INFORMATION .....	42
B. APPENDIX B: NCBI SEQUENCES AND ACCESSION NUMBERS .....	49
C. APPENDIX C: COMPLETE BAYESIAN INFERENCE PHYLOGENETIC TREE.....	52
D. APPENDIX D: COMPLETE MAXIMUM LIKELIHOOD PHYLOGENETIC TREE .....	53
E. APPENDIX E: EPIDEMIOLOGY DATA FOR INFECTED OOCYTES COLLECTED IN 2017 .....	54
REFERENCES CITED.....	55

## LIST OF FIGURES

Figure	Page
1.1 Diagram of microsporidian development. ....	3
1.2 Development of <i>M. alaskensis</i> ploidium .....	5
2.1 Gray scale images of infected <i>M. alaskensis</i> oocytes and released microsporidia .....	9
2.2 Hoechst (fluorescent DNA dye) stained images taken at two focal heights within an infected <i>M. alaskensis</i> oocyte .....	10
2.3 Google Earth maps of collection sites .....	11
2.4 Oocytes observed under DIC light microscopy .....	19
2.5 Selection from the ML tree of 138 microsporidian SSU sequences including the unknown microsporidian from this study .....	21
2.6 Selection from the bayesian inference phylogeny of 138 SSU sequences .....	21
2.7 TEM images of spore filled PSVs .....	22
2.8 Histological images of microsporidian infected female <i>M. alaskensis</i> .....	24
2.9 Neighbor-joining tree of CO1 barcoding results for positive <i>Maculaura</i> hosts with reference sequences from NCBI .....	26
2.10 Development of infected oocytes.....	28
2.11 Time lapse video images of <i>M. alaskensis</i> development from uninfected oocytes (top images) and infected oocytes (bottom images) .....	29
2.12 Hypothesized lifecycle of <i>Oogranate</i> sp. ....	36

## LIST OF TABLES

Table	Page
2.1 List of all primers used for nucleic acid detection and species delimitation. Includes primer name, sequence, target gene, target organism, amplicon size, and references .....	13
2.2 Comparison of biological and morphological features of microsporidia in the family Hepatosporidae .....	32

## CHAPTER 1

### INTRODUCTION

#### Microsporidia

Microsporidia are a peculiar group of eukaryotic spore-forming unicellular organisms that parasitize cells of protists and animals. These organisms were once thought to belong at the base of the eukaryotic tree because their simple cells lack key eukaryotic traits (e.g., mitochondria, cilia). However, their evolutionary history has been shaped by major reductions in their genome and cellular machinery (Corradi, 2015; Keeling & Fast, 2002; Weiss et al., 1999). Microsporidia are highly adapted to a parasitic lifestyle; even their mitochondria have been reduced to mitosomes, organelles devoid of genetic material and incapable of producing ATP (Corradi, 2015; Weiss & Becnel, 2014; Wittner & Weiss, 1999). Recent analyses based on molecular data conclude that Microsporidia are either a sister clade to the Fungi or a basally branching group within the Fungi (Corradi, 2015; Keeling & Fast, 2002; Weiss et al., 1999).

A dormant single-celled spore is both the most recognizable life-stage and the transmissible stage. Like viruses, microsporidia must insert material into host cells to become active and replicate; they achieve this cellular invasion using a unique infection apparatus: the polar tube (Lom & Vavra, 1963; Wittner & Weiss, 1999). Spores contain an atypical Golgi apparatus, ribosomes, a nucleus (or nuclei), a tightly and neatly looped polar tube, a vacuole, an anchoring disc, and a polaroplast (Franzen, 2008; Weiss & Becnel, 2014; Wittner & Weiss, 1999). Spores mature when environmental conditions trigger an explosive eversion of the polar tube with the assistance of the polaroplast and rapid expansion of the vacuole. The rapidly fired polar tube acts as a needle, forcibly

puncturing a host cell and allowing the passage of spore contents (i.e., the nucleus, ribosomes, and sporoplasm) into the cell cytoplasm. Once inside, host ATP and other metabolites are siphoned from the host cytoplasm and used for microsporidian reproduction, protein synthesis, and spore formation (Figure 1.1). Completed spores are released into the surrounding environment, often by cell lysis, where they survive long periods outside of host cells, up to several years in some cases, even in inclement environments (Weiss & Becnel, 2014; Wittner & Weiss, 1999).

Horizontal transmission, whether via dormant spores in the environment or between individual hosts (e.g., during predation), is the most common mode of infection and is achieved by a breach of host epithelial cells. It is the initial or ancestral state and often the host is intensely and negatively affected by parasite growth (Wittner & Weiss, 1999; Weiss & Becnel, 2014). Vertical transmission evolves over many generations of host-microsporidian infections and this lower risk life-history strategy allows for direct passage of microsporidia from adult to offspring (Dunn & Smith, 2001; Ryan & Kohler, 2010).

As in most host-parasite relationships, infection severity is a function of shared evolutionary history between host and parasite (Ryan & Kohler, 2010). Some microsporidian species are commensal with co-evolved hosts while highly pathogenic infections can occur within naïve hosts, even intraspecifically. For example, wild *Caenorhabditis sp.* can carry high loads of the microsporidian *Nematocida parisii* without affecting tissue function, but this same parasite can cause 100% mortality in lab strains of *C. elegans* (Ardila-Garcia & Fast, 2012). Co-evolution between host and pathogen progresses towards a more commensal relationship as observed in *Gammarus*



*duebeni* infected with *Nosema granulosis*, in which infection causes little to no negative effects on the host (Bandi et al., 2001; Ironside et al., 2003). Often, parasites which neutrally or positively impact hosts are vertically transmitted while those causing high morbidity or mortality are horizontally transmitted (Bandi et al., 2001; Dunn & Smith, 2001).

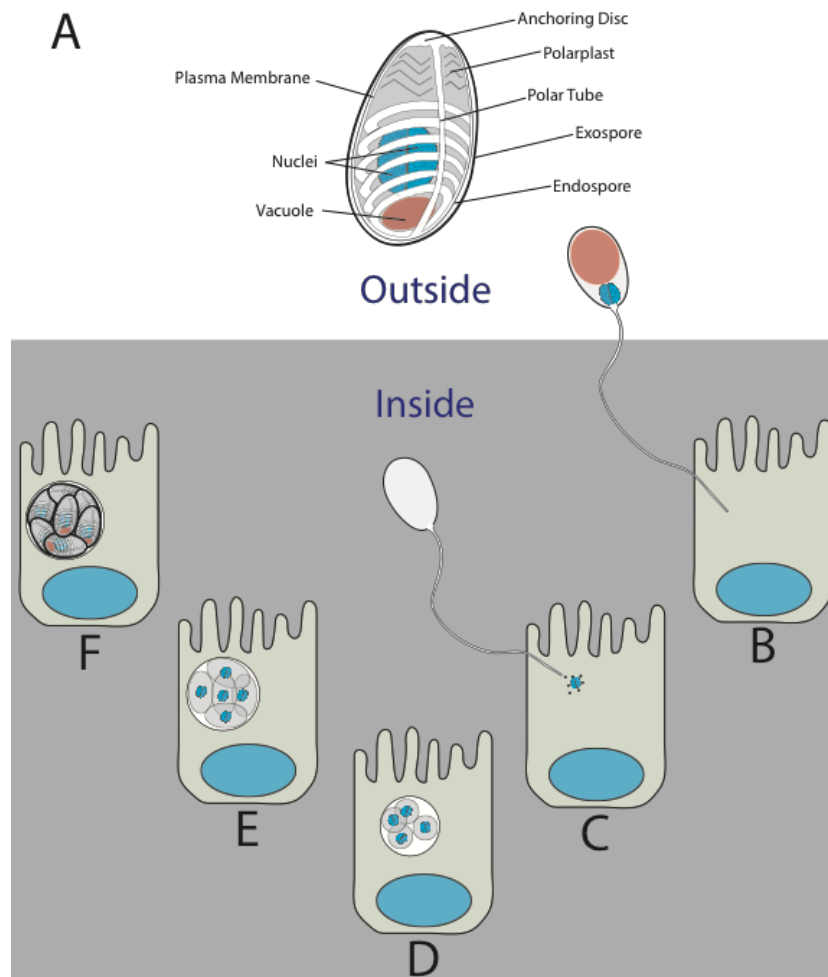


Figure 1.1 – Diagram of microsporidian development. A) The infective (spore) stage. B) Cell maturation triggers polar tube eversion. C) Insertion of spore nuclei and sporoplasm into host cell. D) Merogony, the proliferative stage of the parasite. DNA replication occurs by binary fission (depicted), plasmotomy, or schizogony. E) Sporogony: spore formation begins. Cells grow larger and some continue to divide. Sporonts differentiate into sporoblasts and cease division. F) Spore coat formation completes the lifecycle. Spores are released typically by cell lysis. Modified from Weiss and Becnel 2014.

## Nemertea

The nemertea, or ribbon worms, are a phylum of carnivorous soft-bodied animals defined by a flexible, eversible proboscis that is housed within a fluid filled cavity called the rhynchocoel. Adult nemerteans are voracious predators with few to no known natural enemies; many species secrete a thick mucus imbued with acids and toxins that render them unpalatable. Many nemertean species utilize broadcast spawning, freely releasing gametes into the surrounding water for fertilization and development. Nearly all representatives of this phylum are marine and, like many other marine invertebrates, nemerteans basally have a biphasic lifecycle with free swimming larvae and benthic adults (Stricker, 1992).

Parasites of nemerteans are rarely mentioned in the literature. In a 2006 review of Nemerteans as hosts for symbionts, *Nosemoides vivieri* is the only microsporidian found associated with nemerteans. However, the microsporidian in question is a hyperparasite that infects a gregarine parasitizing nemerteans, and not the nemertean cells themselves (McDermott, 2006; Vinckier, 1975; Vinckier, Devauchelle, & Prensier, 1970).

## *Maculaura*

Nemertean worms of the genus *Maculaura* were formerly known collectively as *Micrura alaskensis*. Genetic data identify five separate species composing this cryptic species complex (*Maculaura alaskensis*, *M. aquilonia*, *M. cerebrosa*, *M. oregonensis*, and *M. magna*) (Hiebert & Maslakova, 2015). All five species co-occur within sandy mudflats along the Pacific coast of North America alongside several other nemerteans. *Maculaura* are pilidiophoran heteronemerteans, a group characterized by the swimming,

planktotrophic pilidium larva which strongly resembles the hat of fictional private investigator, Sherlock Holmes (Figure 1.2A & B). *Maculaura*, like other pilidiophorans, exhibit maximally-indirect development where larval feeding elicits growth and development of juvenile rudiments within but separate from the larval body. Once fully developed, the juvenile worm escapes by rupturing the larval body wall, backing out, and devouring larval tissues as it proceeds in its exodus (Figure 1.2C). The larval body is, typically, consumed entirely, pulled into the mouth shared between larva and juvenile in a catastrophic metamorphosis (Maslakova, 2010).

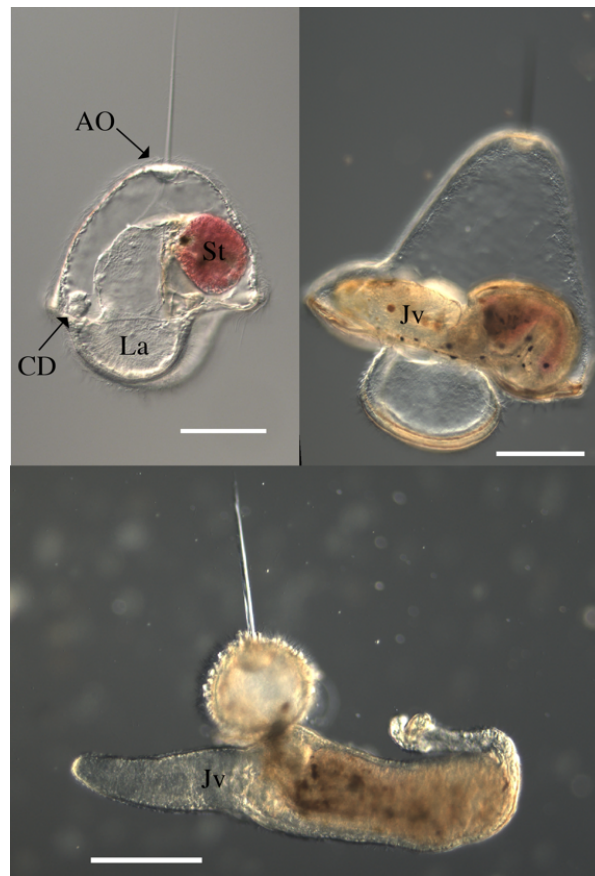


Figure 1.2 – Development of *M. alaskensis* pilidium. Top left – one-week old lab-reared pilidia larva (scale bar 100  $\mu$ m). Top right – 41-day old pilidium with complete juvenile worm inside (scale bar 200  $\mu$ m). Bottom – 41-day old *M. alaskensis* juvenile engulfing the larval body during metamorphosis (scale bar 200  $\mu$ m). Apical organ (AO), stomach (St) pigmented by algal prey, lateral lappets (La), one of a pair of cephalic discs (CD): the first set of juvenile rudiments to form, and juvenile (Jv).

*M. alaskensis* is a model system for cellular, developmental, and evolutionary biology (Bird, von Dassow, & Maslakova, 2014; Hiebert & Maslakova, 2015; Maslakova, 2010; von Dassow & Maslakova, 2017). Ripe adult specimens are readily available in an adequate environment; fertilization and subsequent development occurs consistently in a laboratory setting. Additionally, an unknown microsporidian infection was first observed within oocytes of *M. alaskensis* by Drs. George von Dassow and Svetlana Maslakova. This study is a species description of that previously undescribed microsporidian and an examination of the host-parasite relationship particularly as it relates to development of infected oocytes.

## CHAPTER 2

### HEPATOSPORIDAE N. GEN., N. SP., A MICROSPORIDIAN PARASITE OF RIBBON WORMS IN THE GENUS *MACULAURA* ON THE EASTERN PACIFIC COAST

#### Introduction

Microsporidia are spore-forming obligate intracellular parasites which are a sister clade to - or a basally branching group of - fungi (Corradi & Keeling, 2009; Keeling & Fast, 2002). These specialized parasites have been found infecting protists and the cells of nearly every phylum of animal (Weiss & Becnel, 2014; Wittner & Weiss, 1999). At present, 200 genera have been discovered and approximately 1,400 species have been described (Weiss & Becnel, 2014). Of these described genera, roughly 50 infect aquatic arthropods, and 21 infect other marine invertebrates and protists (Stentiford et al., 2013). These numbers certainly underestimate the real diversity of this group due to their infectivity rates and the prevalence of spores in nature. Some species of microsporidia are capable of infecting multiple host species and there are hosts that are susceptible to more than one microsporidian. For these reasons, microsporidian biologists hypothesize at least one microsporidian parasite for each species of animal on earth (Keeling and Fast, 2002). Under-documentation is problematic as these parasites are likely a major influence shaping organismal biology and ecosystem dynamics.

Ribosomal gene sequences have been used for diagnosis and to establish modern microsporidian taxonomies (Vossbrinck & Debrunner-Vossbrinck, 2005; Weiss & Becnel, 2014; Wittner & Weiss, 1999). There are over 4,000 partial or complete small subunit ribosomal RNA (SSU) reference sequences available for Microsporidia in

Genbank (<https://www.ncbi.nlm.nih.gov/genbank/>). Phylogenetic analyses of the SSU genes reveal five distinct clades (Vossbrinck & Debrunner-Vossbrinck, 2005). Clade IV is composed almost entirely of parasites of aquatic crustaceans and fish, with one notable exception: *Enterocytozoon bieneusi* is the most common cause of microsporidiosis in immunocompromised human patients and is thought to be a zoonotic disease (Stentiford et al., 2011). Within Clade IV, the family Hepatosporidae has been tentatively proposed following the discovery of *Hepatospora eriocheir*, a microsporidian infecting Chinese Mitten Crabs in Europe (Stentiford et al., 2011; Wang & Chen, 2007). *H. eriocheir* is the sole member of this sister family to the Enterocytozoonidae (Bojko et al., 2017; Stentiford et al., 2011).

Here we describe a new microsporidian infecting oocytes of nemerteans, or ribbon worms, in the genus *Macaulaura* on the Pacific coast of North America. *Macaulaura* live under rocks and in sand within tidal mudflats exclusively in marine and estuarine environments (Hiebert & Maslakova, 2015). These worms range from Alaska to Southern California and have also been found in the Sea of Okhotsk in Russia (Coe, 1905; Hiebert & Maslakova, 2015). We find, with some frequency, oocytes from *M. alaskensis* or *M. aquilonia* containing large vesicles filled with small refractive ovoid objects that have diplokaryotic nuclei (Figure 2.1 and 2.2). We have determined these vesicles contain spores from a previously undescribed microsporidian that is a new representative of the family Hepatosporidae based on analysis of phylogenetic and morphological evidence. This is, to our knowledge, the first species of microsporidia found to directly infect a nemertean host.

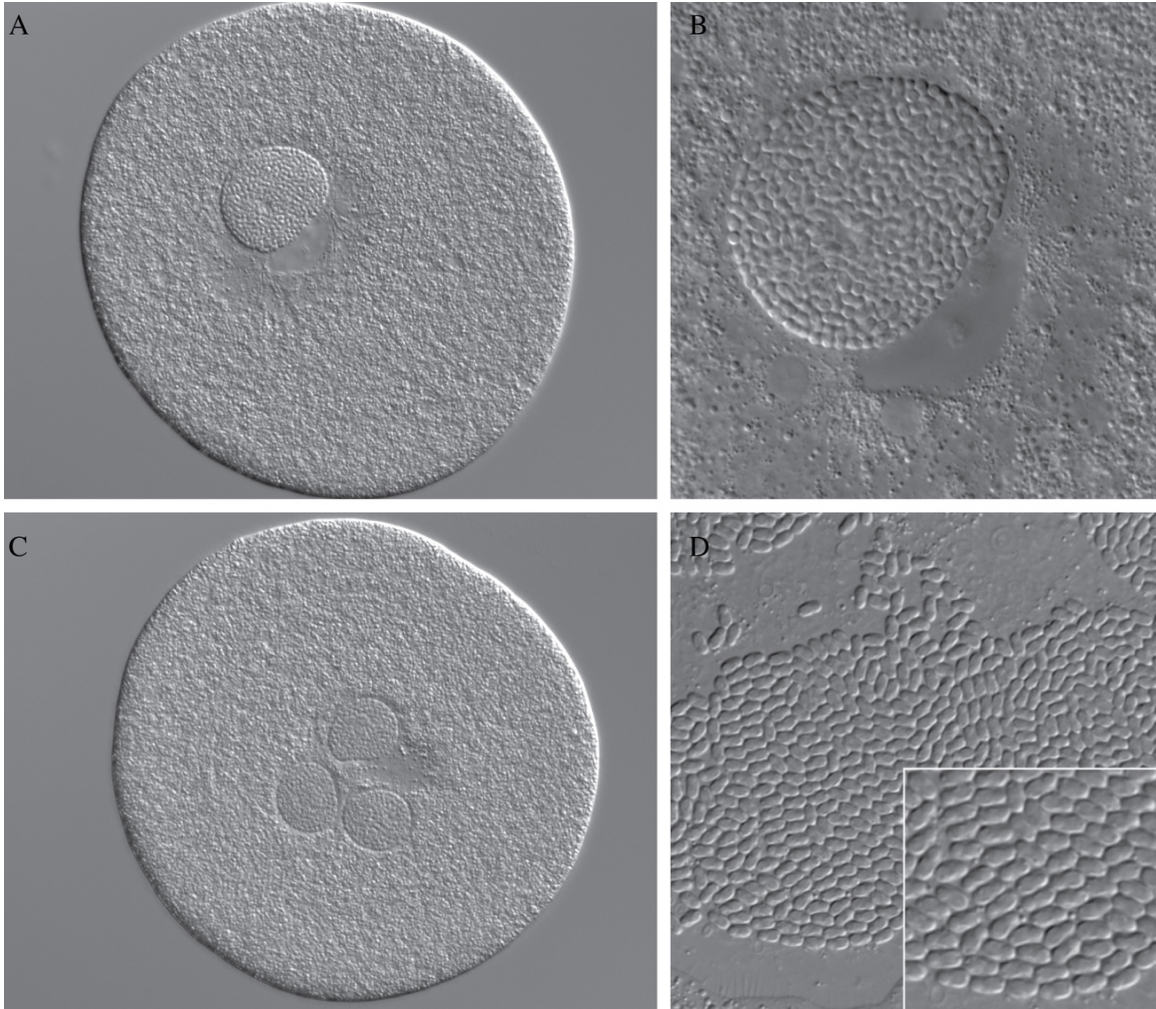


Figure 2.1 – Gray scale images of infected *M. alaskensis* oocytes and released microsporidia. A, C) Infected oocyte images. Oocytes with distinct vesicles containing refractile oval objects compressed tightly under a cover slip. B) Vesicle from image A at higher magnification. C) Objects from image B released from PSV by compression, each with distinct internal structure. Images by George von Dassow, unpublished data.

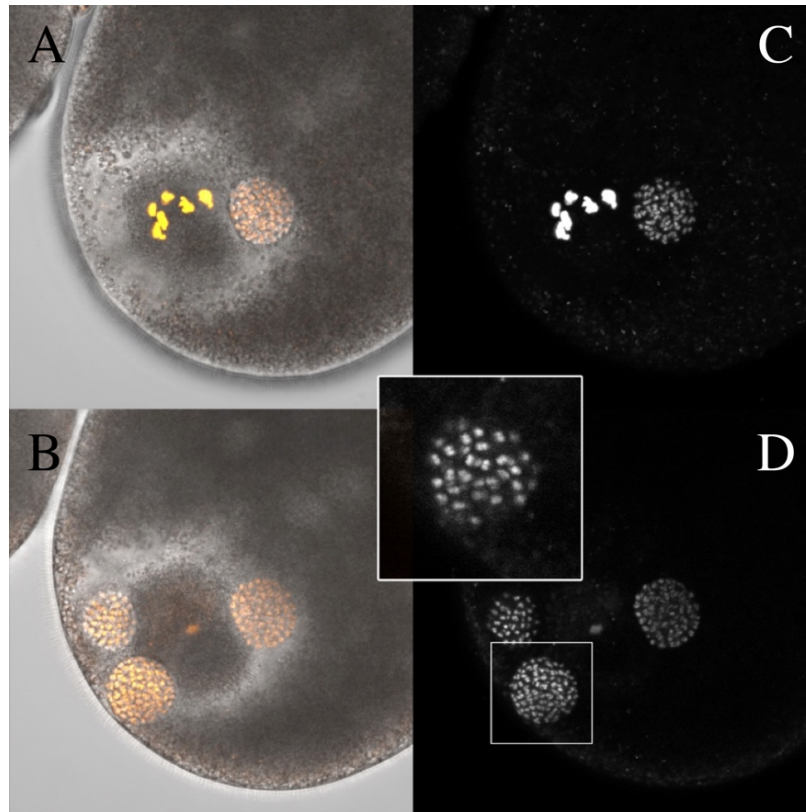


Figure 2.2 – Hoechst (fluorescent DNA dye) stained images taken at two focal heights within an infected *M. alaskensis* oocyte. A, B) Images taken with fluorescent light overlaying transmitted light. C, D) Same as pictured in A and B with fluorescent light only. Inset image shows distinct diplokarya. Images by George von Dassow, unpublished data.

## Materials and Methods

### *Collections*

Live adult *Maculaura* and other nemerteans were collected from sandy mudflats using shovel and hand collection between July 2016 and October 2018 (ODFW collecting permits 202453, 21204, and 21962). The specimens came from mudflats we refer to as Portside (43°20'33 N, 124°19'27" W), Fisherman's Grotto (43°20'32" N, 124°19'5" W), and Metcalf Marsh (43°20'10" N, 124°19'33 W) in Charleston, Oregon and Hatfield Marsh (44°37'4' N, 124° 2'40" W) in Newport, Oregon (Figure 2.3 and Appendix A). In the laboratory, individual *Maculaura* were separated into finger bowls filled with sea



water filtered to 0.2  $\mu\text{m}$  (FSW). Other nemerteans were separated into bowls based on morphological features. All bowls were kept immersed in flowing seawater tables at ambient water temperature 13-18° C. Each *Maculaura* was given a unique designation and used for the following experiments. Adult *Maculaura aquilonia* tissue samples collected from Juneau, Alaska by Terra Hiebert in August of 2014 and preserved in 95% ethanol at -20° C were included in this study (Figure 2.3 and Appendix A). Experiments were performed at the Oregon Institute of Marine Biology unless otherwise indicated.

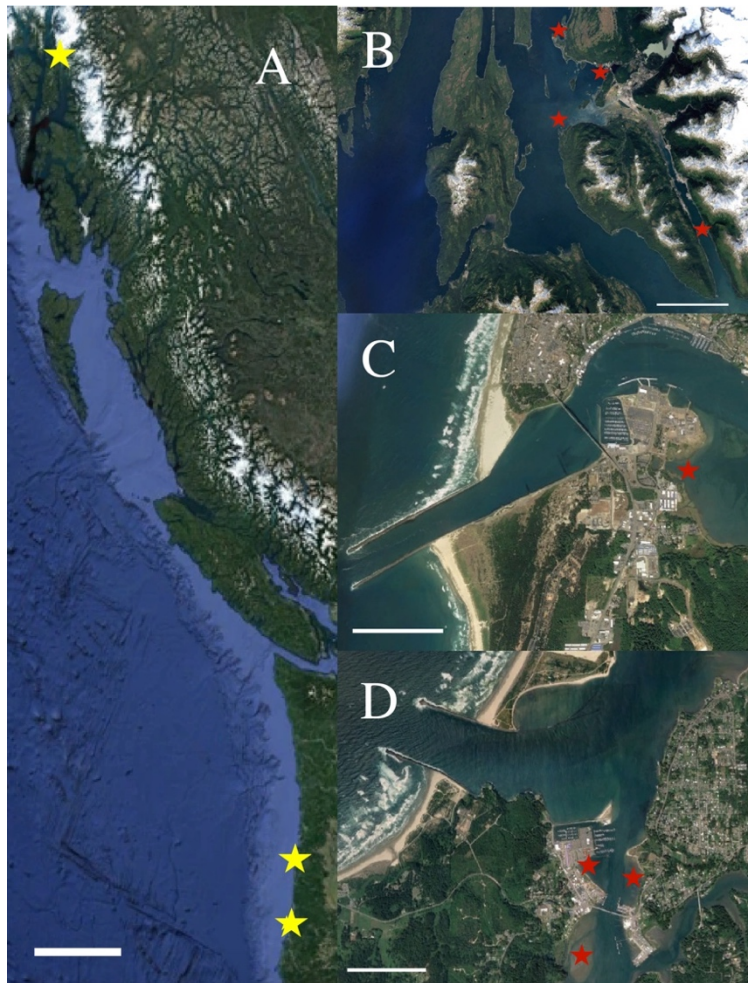


Figure 2.3 – Google Earth maps of collection sites. A) Pacific Coast map of sampling locations; scale bar is 160 km. B) Juneau, Alaska 2014 from North to South: Lena Beach, Auke Bay, Outer Point, and Sheep Creek; scale bar is 8 km. C-D) Scale bar is 0.8 km. C) Hatfield Marsh in Yaquina Bay, Newport, Oregon. D) Coos Bay, Oregon from North to South: Portside (left), Fisherman’s Grotto (right), and Metcalf Marsh.

### *Light Microscopy Analysis*

Ripe female *M. alaskensis*, *M. aquilonia*, *M. magna*, and *M. cerebrosa* were placed in a petri dish with FSW. Ripe female *M. oregonensis* were not available for observation. A 1 cm segment was removed from the posterior end and oocytes were released from ovaries using a razor blade and fine forceps. Oocytes were examined under differential interference contrast (DIC) microscopy for overt signs of infection. Infected oocytes were analyzed for measurable characters including number of infected oocytes from a single female as well as parasitophorous vesicle (PSV) number and size.

### *DNA Extraction, PCR, and Sequencing*

Visibly infected oocytes were collected in sets of 100 oocytes and frozen at -80° C for subsequent PCR testing. Samples were extracted using the QIAamp Biotic Bacteremia DNA Kit (Qiagen #12240-50) with the following adjustments. A 0.5 mm PowerBead Tube (Qiagen #13116-50) was used for the first incubation and subsequent vortexing step. Oocytes were incubated in Buffer MBL at 70° C for 20 minutes mixing at 1,400 rpm in a Thermomixer heating block.

Universal microsporidian primers for the small subunit ribosomal RNA (SSU) and RNA Polymerase II (RPB1) genes were used to amplify DNA from the unknown microsporidia (See Table 2.1). All PCR reactions used GoTaq DNA polymerase (Promega #M3005) using kit recommendations with the following variable parameters: 0.5µM or 1 µM of each primer, and 2 µL of template DNA. Reactions used an elongation step of 1 minute and 10 seconds with an annealing temperature of 56°C for RPB1 and 43°C for SSU.

Table 2.1 – List of all primers used for nucleic acid detection and species delimitation. Includes primer name, sequence, target gene, target organism, amplicon size, and references.

Primer or Probe	Sequence	Gene	Target Organism	Amplicon Size	Reference
ss18f ss1492r	5'-CACCAGGTTGATTCTGCC-3' 5'-GGTTACCTTGTTACGACTT-3'	SSU	Microsporidia	1,300 bp	Weiss and Vossbrinck 1999
ss350r* ss1061f*	5'-TTTCGCGCCTGCTGCCSTCCTTG-3' 5'GGTGGTGCATGGCCG-3'	SSU	Microsporidia	-	Weiss and Vossbrinck 1999
RPB1-F1 RPB1-R1	5'-CGGACTTYGAYGGNGAYGARATGA-3' 5'CCCCKNCCNCCCATNGCRTGAAA-3'	RPB1	Microsporidia	1,000 bp	Hirt et al. 1999
MaMicroF2 MaMicroR2	5'-TGTAGGGGGAACGACAAACAGCTCAG-3' 5'-TTGCACTTGTAGCCCAAACCATCTGAGAG-3'	SSU	Hepatosporidae n. gen., n. sp.	900 bp	This study
LCO1490 HCO2198	5'-GGTCAACAAATCATAAAGATATTGG-3' 5'TAAACTTCAGGGTGACCAAAAAATCA-3'	COI	Nemertean	658 bp	Folmer et al. 1994

\*Primers used for sequencing only

PCR products were inserted into pGEMT+ Vector Systems (Promega #A3600) and grown with Subcloning Efficiency DH5a cells (Invitrogen #18265017). Colonies were selected and reamplified with universal primers. Following purification with the Wizard SV Gel and PCR Clean-up Kit (Promega # A9282), products were sent to Sequetech Corporation (Mountain View, California) for single primer extension Sanger Sequencing. The resulting chromatograms were trimmed and aligned using Geneious software version 11.0.4. Resulting consensus full length sequences were run through BLASTn and BLASTx databases.

### *SSU Phylogenetic Analysis*

For phylogenetic analysis, an additional 137 microsporidian SSU sequences were downloaded from the NCBI database with emphasis on microsporidia Clade IV

(Appendix B for NCBI reference sequences list) (Vossbrinck & Debrunner-Vossbrinck, 2005). These sequences plus the full-length consensus SSU sequence for the unknown microsporidian were assembled with a MAFFT alignment in Geneious. J-Model Test was used to determine the best fit model for maximum likelihood (ML). The ML tree was built in Geneious using Phyml with a GTR+I+G Model using 200 bootstrap replicates. The same alignment and model were used to create a bayesian inference phylogeny within Geneious.

### *Transmission Electron Microscopy (TEM)*

Some visibly infected oocytes were fixed in 2% glutaraldehyde (Electron Microscopy Sciences [EMS] #16316) in 0.2 M sodium cacodylate buffer (SCB) (EMS #11650) for 1 hour, rinsed three times in SCB, post-fixed in 2% osmium tetroxide (EMS #19150) in SCB for one hour, and dehydrated through a graded ethanol series (Bozzola & Russell, 1999). At the Center for Advanced Materials Characterization (CAMCOR) at the University of Oregon Eugene Campus, oocytes were infused with LR white resin (EMS #14380) using a resin to ethanol dilution series (1:3 once, 2:3 once, 100% resin twice; incubating 30 minutes for each step) then embedded in LR white resin plus LR accelerant. Blocks were set at 4°C for 30 minutes prior to sectioning. Ultra-thin sections, approximately 90-100 nm thick, were prepared with freshly broken glass knives on an LKB Ultramicrotome III and mounted on uncoated 300 mesh copper grids. Sections were stained with 4% uranyl acetate and Reynold's lead citrate (Reynolds, 1963) then imaged with the FEI Tecnai G2 Spirit TEM.

## *Histology*

Tissues from adult female *Maculaura* with visibly infected oocytes, females with visibly uninfected oocytes, and adult male *Maculaura* were fixed and stained for histological examination. Specimens were relaxed in a 1:1 mixture of 0.33 M MgCl<sub>2</sub> and FSW at 4°C (30 minutes), fixed with 10% formalin in phosphate buffered saline (PBS) (24 hours), post-fixed in Hollande's Bouin fixative (72 hours), rinsed in RO water, dehydrated with an ethanol series (10% EtOH, 30% EtOH, 50% EtOH, and 70% EtOH for 10 minutes each), and rinsed daily for one week with 70% ethanol. Tissues were stored in 70% ethanol for further processing.

At the University of Oregon Histology Laboratory, samples were dehydrated, cleared, and paraffinized in an automated tissue processor by the following process: ethanol dehydration (70% EtOH, 80% EtOH, 95% EtOH twice for 10 minutes each followed by 100% EtOH twice for 20 minutes each), xylene (20 minutes), Clear-Rite 3 (20 minutes), Paraffin Type 6 (25 minutes twice), Paraffin Type 9 (25 minutes), and a final change of Paraffin Type 9 (all reagents used during tissue processing came from Richard-Allan Scientific). Samples were embedded in Paraffin Type 9 (56°C melting point), sectioned at 7 µm thickness, and mounted on glass slides.

Following deparaffinization, slides were stained with Weber's Chromotrope (6 g chromotrope 2R, 0.15 g fast green, and 0.7 g phosphotungstic acid in 3 mL glacial acetic acid) (Weber et al., 1992; Weiss & Becnel, 2014). Stained slides were cleared in xylene, mounted with PermOUNT mounting medium (EMS #17986), and examined with an Olympus DIC microscope. Histology images were taken using a SPOT imaging camera and software.

### *Larval Development Observations*

*M. alaskensis* oocytes with a fraction of individuals containing conspicuous PSVs in the cytoplasm were allowed to mature in FSW for 1 hour then fertilized in FSW within a Syracuse dish treated with Bovine Serum Albumin (BSA) to prevent sticking. Five minutes after fertilization, zygotes were mounted on a glass-bottom Petri dish. Time lapse videos were taken on a Leica DMI8 inverted microscope with a cooling stage set at 15°C. StreamPix software recorded videos at 1 frame every 12 seconds. Development was recorded until the hatching of swimming blastosquares, a specialized flattened blastula characteristic for *M. alaskensis* development (Maslakova, 2010). Control videos were taken of oocytes from visibly uninfected *M. alaskensis* under the same conditions.

*M. alaskensis* larvae from females carrying some fraction of infected oocytes were grown in 150 mL finger bowls filled with FSW, and set in running sea water tables at 13-18° C. Cultures were cleaned every three days and fed cultured *Rhodomonas lens* throughout development. At 7, 14, 30, and 40 days of development individuals were photographed and frozen at -80° C for PCR testing. Additionally, following metamorphosis (between 36 and 41 days), juveniles were collected, frozen, and PCR tested for infection.

### *Diagnostic PCR for Detection of Hepatosporidae n. gen, n. sp.*

A species-specific primer set was designed to amplify a 900-base pair fragment of the SSU sequence of the unknown microsporidian (Table 2.1). Live adult *Maculaura* collected between January and October of 2018 were examined for their reproductive

status (not ripe, ripe female, ripe male), then a 2-3 mm<sup>3</sup> cross-section was removed from the posterior 1/3 of the animal and frozen at -80° C. To survey the infection status of nemerteans other than *Maculaura* collected from the same habitat, nemertean tissues were pooled by species. For these nemerteans a small cross-section was cut from each animal (up to 8 animals in one pool) and frozen together as one sample (Appendix A includes collection and samples details). Between animals, tools and petri dishes were washed with 10% bleach, rinsed in RO water, UV treated for 20 minutes on each side, then washed and rinsed in a separate 10% bleach and RO container to prevent cross contamination. Larvae and newly metamorphosed juveniles from the developmental studies along with the preserved adult specimens from Juneau, Alaska in 2014 were also tested.

Adult tissues frozen in FSW were removed from the freezer and rinsed once in nuclease-free water prior to DNA extraction. Samples stored in ethanol were rinsed three times in 1 mL nuclease-free water over 10 minutes before extraction. Following rinsing, adult tissues were ground with a plastic pestle in a microcentrifuge tube. All samples were extracted using the QIAamp Biostic Bacteremia DNA Kit and following the protocol described previously. Larvae and new juveniles were extracted using 1/4 volume of glass beads and 1/3 volume of Buffer MBL, IRS, and BB. All other volumes remained the same. PCR were performed using GoTaq DNA Polymerase under kit conditions with 0.5µM of each primer and 2 - 8 µL of template DNA. Cycling conditions involved annealing temperatures between 52° and 56° C and elongation time of 55 seconds. All PCR were checked for a positive reaction by gel electrophoresis. Of the samples which produced a band of the expected size, 40% were purified and sent for sequencing.

### *DNA Barcoding of Infected Nemerteans*

All adult DNA samples which tested positive for microsporidian infection by PCR were subjected to a PCR test with “universal” metazoan CO1 primers (Folmer et al., 1994) for host identification. Reactions were run as above with the following exceptions: 2 µL of template DNA, annealing temperature of 45° C, and elongation time of 1 minute. Samples were purified and sequenced by Sequetech Corporation. The resulting sequences were analyzed using BLASTn for initial identification, then compared with reference sequences from each of the five described species of *Maculaura* and an outgroup downloaded from the NCBI database. All samples and reference sequences were assembled using the Geneious alignment under default settings and a neighbor-joining tree was built from the result.

## RESULTS

### *Light Microscopy Observations*

Oocyte infections exhibiting cytoplasmic parasitophorous vesicles (PSVs) were observed in *M. alaskensis* and *M. aquilonia* (Figure 2.4) but not found in *M. cerebrosa* or *M. magna* (*M. oregonensis* oocytes were not observed). Additionally, infected *M. alaskensis* oocytes sometimes exhibited a thick chorion-like layer surrounding the oocyte surface, a feature not typically present in this species (Figure 2.4 D). From four infected female *M. alaskensis*, oocytes contained anywhere from one to twelve PSVs in the cytoplasm with an average of 2.36 PSVs per infected oocyte. Oocytes from an infected female with visible spore-filled vesicles ranged from 5 to 15.8 percent of the total number of oocytes (Appendix E). The size of the PSV and the number of spores contained within



the vesicles varied dramatically: PSV diameters ranged from 6 to 30  $\mu\text{m}$  so volumes range from 0.1 – 10 picoliters. Earlier life stages were also observed within PSVs, but at a much lower frequency than spore-filled vesicles (Figure 2.4 D).

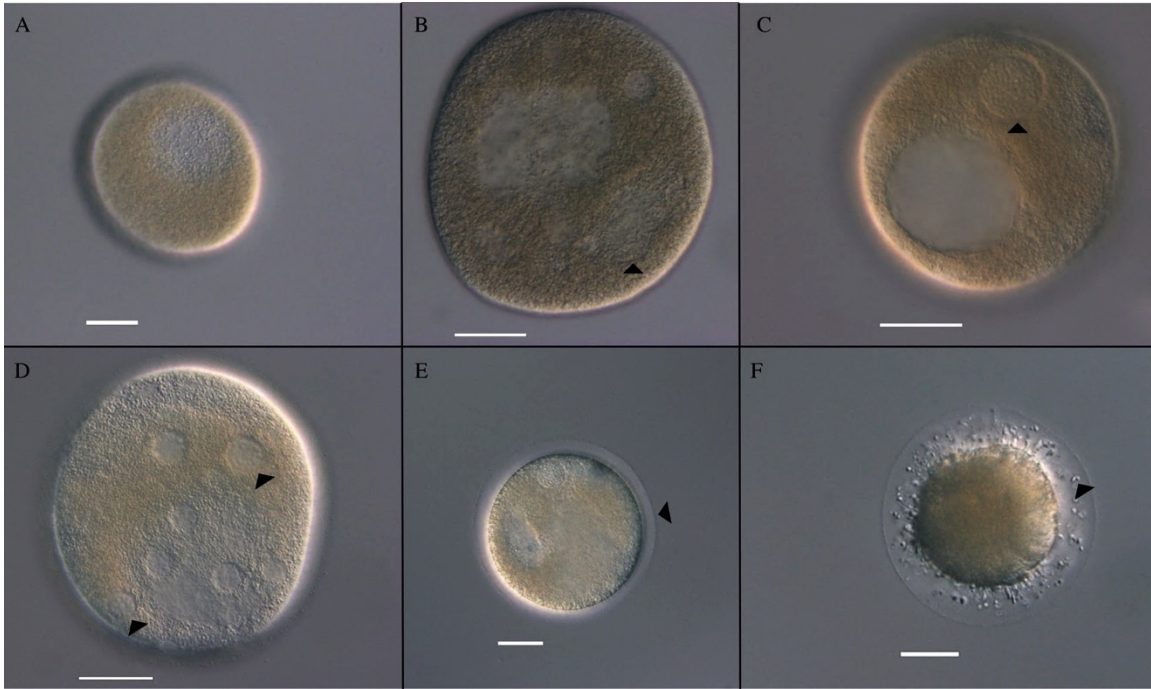


Figure 2.4 – Oocytes observed under DIC light microscopy. A) Healthy *M. alaskensis* oocyte. B) Hypothesized infected oocyte of *M. alaskensis*, containing large vesicles and exhibiting cytoplasmic clearing (arrowhead) but no obvious spore-filled vesicles C) *M. alaskensis* oocyte with a large PSV containing distinct spores (arrowhead). D) *M. aquilonia* oocyte containing several PSVs with developing sporoblasts inside (arrowheads). E) *M. alaskensis* oocyte with a distinct chorion-like layer (arrowhead), a feature not typically found surrounding oocytes of this species, and a visible PSV. F) Infected *M. alaskensis* oocyte with numerous unidentified objects (arrowhead) occupying the space between the oocyte surface and the chorion-like layer. PSV present but not visible in this image. All scale bars 25  $\mu\text{m}$ .

#### *SSU and RPBI Sequencing*

A 1,280 basepair small subunit ribosomal RNA (SSU) consensus sequence was used for identification. The sequence had a 73% identity match to *Microsporidia* sp. DP-

1-19 (NCBI Accession AF394528) with 95% query coverage suggesting this organism belongs within Clade IV and class Terresporidia (Vossbrinck & Debrunner-Vossbrinck, 2005). It also suggests this species is separate from all other species represented in GenBank.

The resulting 888 basepair RPB1 sequence had a query coverage no higher than 15% when analyzed with BLASTn. Using BLASTx, the protein sequence matched *Hepatospora eriocheir* (98% query coverage and 57% identity), another member of Clade IV and within the proposed family Hepatosporidae (Bojko et al., 2017; Stentiford et al., 2011; Wang & Chen, 2007). This provides additional evidence the sequence belongs to an undescribed microsporidian within Clade IV.

#### *SSU Phylogenetic Analysis*

Maximum likelihood and Bayesian inference phylogenies group the unknown microsporidian in Clade IV within the suggested family Hepatosporidae with strong support (100% bootstrap and 1.0 posterior probability). The unknown microsporidian and *H. eriocheir* form a sister clade to the Enterocytozoonidae with a posterior probability of 1.0 and 70% bootstrap support (Figure 2.5, Figure 2.6, Appendix C, Appendix D). This gives high confidence in its position in relation to *H. eriocheir* and the other *Enterocytozoon*-like microsporidia.

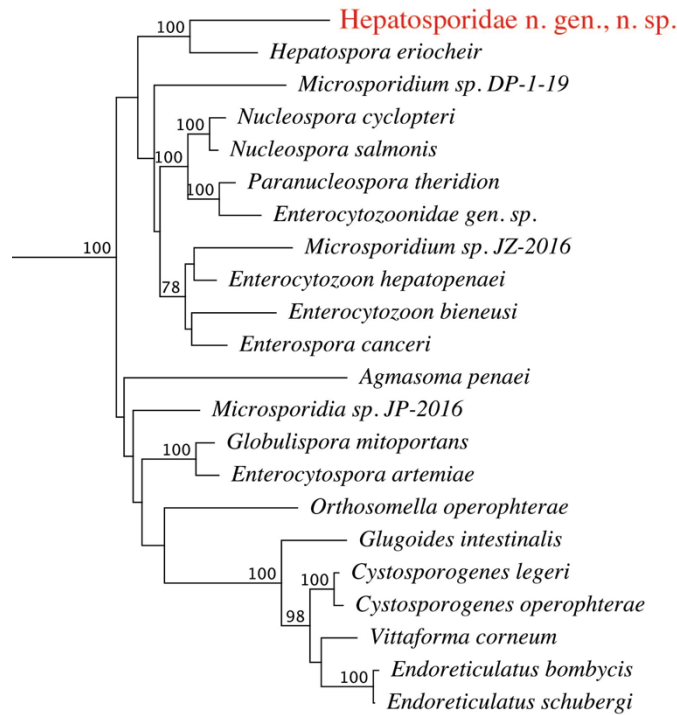


Figure 2.5 – Selection from the ML tree of 138 microsporidian SSU sequences including the unknown microsporidian from this study. Bootstrap support values less than 50 were not included.

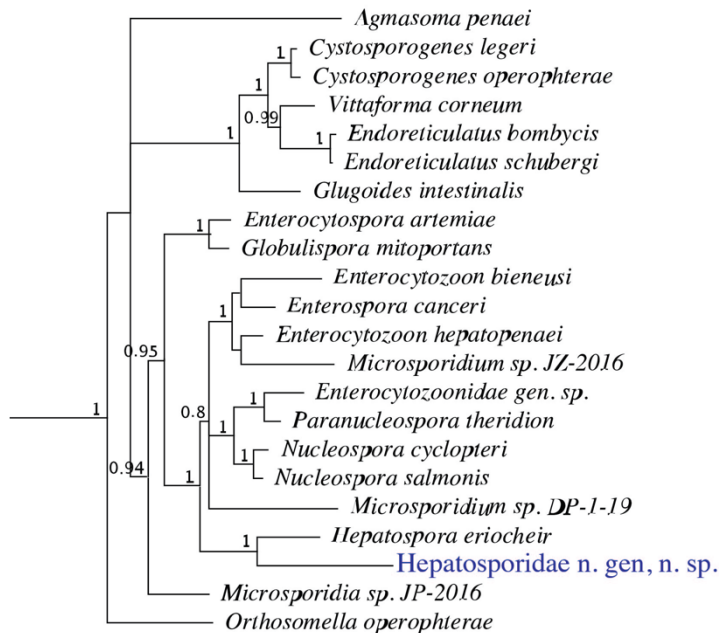


Figure 2.6 – Selection from the bayesian inference phylogeny of 138 SSU sequences. Posterior probabilities lower than 0.5 were not included.

## TEM

The spores are coated with an electron dense exospore, an electron lucent endospore, and a plasma membrane (Figure 2.7). Spores also contain a polar tube, polaroplast, anchoring disc, two nuclei, and a posterior vacuole (Figure 2.7A). The polar tube measures 80 nm in diameter and is arranged in a single layer of six to seven coils. Spores are 2.3  $\mu\text{m}$  long and 1.3  $\mu\text{m}$  wide on average. In one case, vesicles were observed docking or leaving the PSV (Figure 2.7A). Complete spores were always found within a PSV and earlier life stages were not observed with TEM. In one case, a single matured spore with an extended polar tube was found inside a PSV (Figure 2.7B).

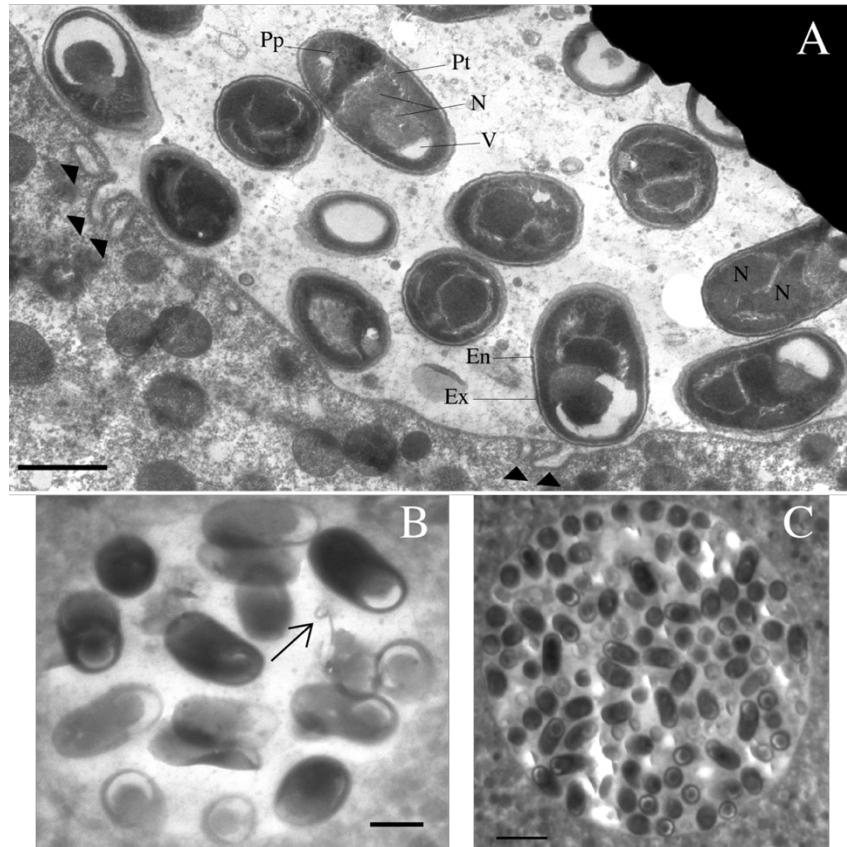


Figure 2.7 – TEM images of spore filled PSVs. A-B) scale bars 1  $\mu\text{m}$ . A) Electron dense exospore (Ex) and electron lucent endospore (En), polaroplast (Pp), nuclei (N), vacuole (V), and cut polar tube (Pt). Vesicles docking or leaving PSV (arrowheads). B) Mature spore with extended polar tube (arrow). C) Densely packed PSV. Scale bar 3  $\mu\text{m}$ .

## *Histology*

Weber's Chromotrope stained the electron dense exospores bright red. Each spore had a visible, uniform internal structure (Figure 2.8A inset). Other life stages of the parasite were also visible and stained blue. The earliest life stages (the meronts) were solid blue without discernable internal structure (Figure 2.8C). Sporoblasts were distinct blue oval objects with obvious internal structure but are missing the spore coat which stains bright red with chromotrope 2R (Figure 2.8D inset). Areas of cytoplasmic clearing could be seen in infected and uninfected oocytes but did not appear to contain any signs of microsporidia (Figure 2.8 A,B,C). Individual oocytes were found carrying multiple separate PSVs at different stages of microsporidian development (Figure 2.8 B,C,D). Often, nearly all oocytes in a single ovary would be infected while the next ovary would have no signs of infection.

Nemertean muscles, epithelium, and other tissue layers of the adult *Maculaura* stained blue. Other features in the epithelial tissue and dermal layers of *Maculaura* stained bright red but were distinguished from microsporidian spores by their lack of distinctive internal features. No signs of microsporidian infection were observed within the adult tissues. Using the histology technique described here, infections were only observed within PSVs of infected oocytes.

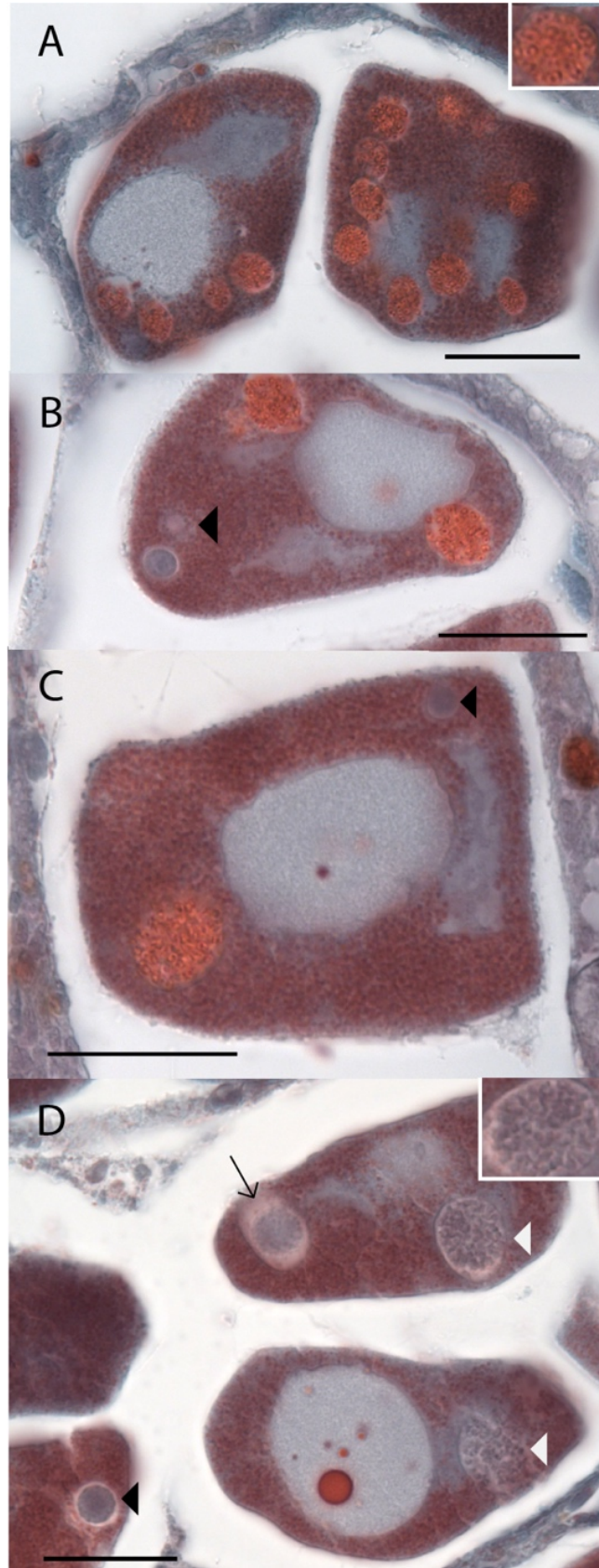
Figure 2.8 – Histological images of microsporidian infected female *M. alaskensis*.

A) Two heavily infected oocytes with multiple separate infections. All PSVs are circular and filled with bright red spores.

B) Oocyte with several PSVs in different stages of development. PSV contained site of early microsporidian development (arrowhead).

C) Infected oocyte with 2 PSVs, one containing spores the other containing a solid blue object with no visible divisions (arrowhead).

D) Ovary with several infected oocytes containing multiple microsporidian infections at different stages of development. Small cells compressed tightly staining blue (black arrowhead). Cells becoming larger and clearly separated with PSV expansion exhibited by clear ring surrounding the developing microsporidia (arrow). Multiple large and discrete cells with visible internal structure (white arrowheads and inset image).



### *Diagnostic PCR and Nemertean Host Barcoding*

Between January and October of 2018, a total of 70 adult *Maculaura* worms from Charleston, Oregon were tested for microsporidia by PCR with species specific primers. Of these, 33 tested positive and produced a visible band by gel electrophoresis. Positive individuals included ripe females, ripe males, and individuals without ripe gametes. They also included representatives from four of five species of the genus *Maculaura*: *M. alaskensis*, *M. aquilonia*, *M. oregonensis*, and *M. cerebrosa*. All three samples from the fifth species, *M. magna*, tested negative for the parasite. Of the Charleston *Maculaura*, 41.4% tested positive for infection by PCR. Excluding *M. magna*, 43.3% of Charleston *Maculaura* tested positive. No other species of adult nemertean collected from Charleston, Oregon tested positive for the unknown microsporidia. Specimens tested included 3 pools of 20 *Cerebratulus* sp. and 1 pool each of the following: 4 *Paranemertes* sp., 4 *Emplectonema* sp., 3 *Carinoma* sp., and 3 *Lineus* sp. “red”.

Of the 17 samples collected from Newport, Oregon, two *M. alaskensis* tested positive. All the worms collected from Alaska in 2014 were previously identified as *M. aquilonia* by Terra Hiebert (Hiebert & Maslakova, 2015). Of the 25 samples of *M. aquilonia*, six tested positive. All samples sent for sequencing came back as a 99% to 100% match to the original consensus SSU sequence and to each other regardless of host species or sampling location. The phylogenetic tree of adult nemertean CO1 sequences (Figure 2.9) confirms the results obtained from BLASTn. In summary, we positively detected the same novel microsporidian in males, females, and unripe individuals of four out of five *Maculaura* species from three distinct locations; limited sampling so far fails to detect its presence in other co-occurring nemertean species.

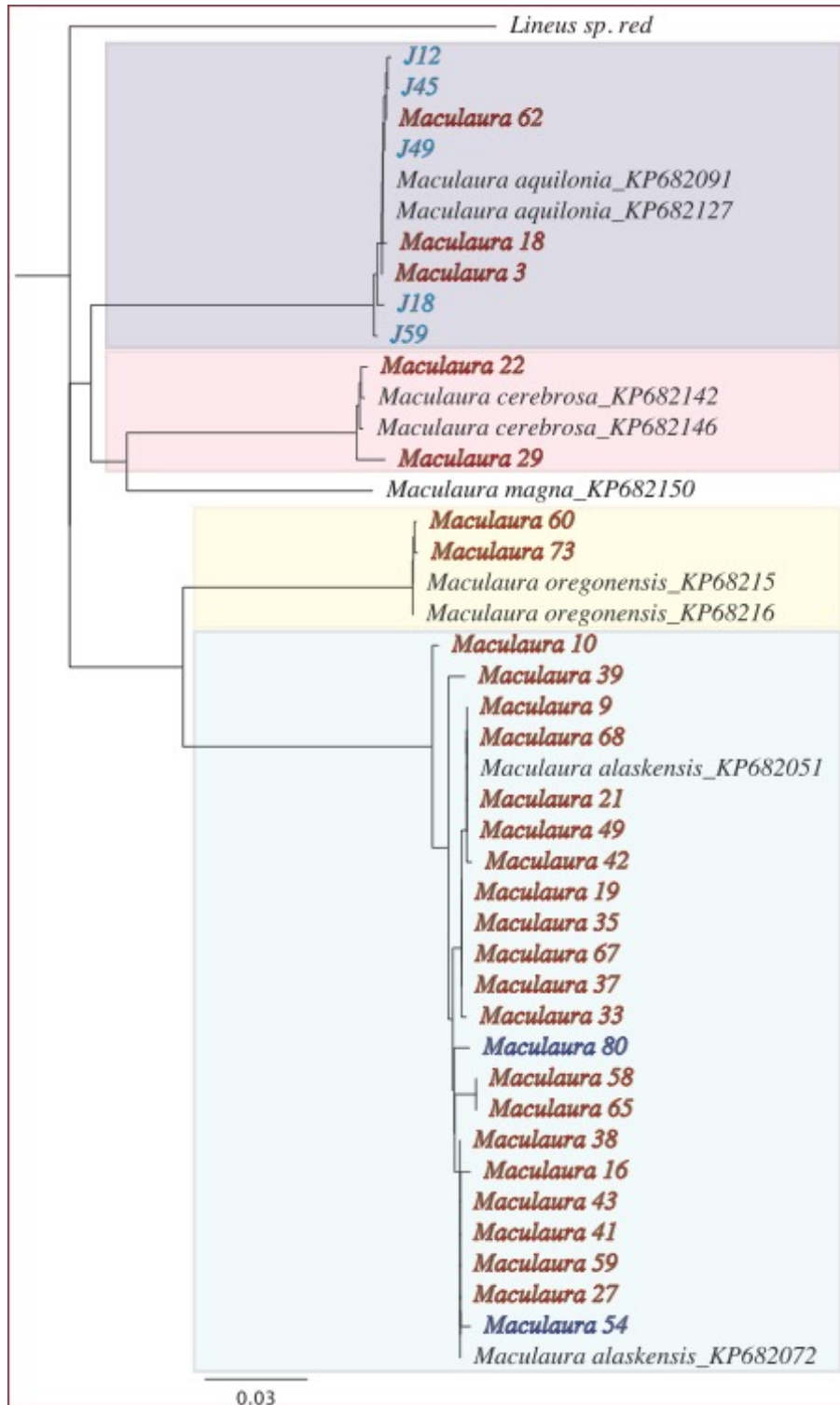


Figure 2.9 – Neighbor-joining tree of CO1 barcoding results for positive *Macaulaura* hosts with reference sequences from NCBI. Clades are color coded and ordered from top to bottom as follows: *M. aquilonia*, *M. cerebrosa*, *M. oregonensis*, and *M. alaskensis*. Specimen colors indicate location of collection site: light blue for Alaska, red for Coos Bay, and dark blue for Newport Oregon.



### *Developmental Studies*

Infection does not entirely prevent apparently normal development. Some fraction of infected oocytes, even those containing numerous or large PSVs, were capable of maturing, fertilizing, and developing into swimming and feeding pilidia (Figure 2.10) while other heavily infected oocytes failed to mature or fertilize. *M. alaskensis* eggs with a chorion-like layer surrounding the surface were also capable of fertilization and could complete development to hatching in some cases. Uninfected embryos showed some uniformity in time to initial cleavage as well as in time spent cleaving through the first five cleavage cycles (Figure 2.11 top images). In the infected embryos, time to first cleavage and time spent cleaving was variable among individuals. Most embryos from this infected female still completed development to hatching without obvious delay when compared with their uninfected counter parts.

In one video, two infected embryos were obviously delayed to first cleavage and took more time to complete cleavage than others in the same group (Figure 2.11 lower images). Cleavage occurred unevenly between separate blastomeres starting in second cleavage in both embryos. Other embryos did not exhibit such blatant non-uniform cell cleavage until later in development. One of these individuals had significantly delayed development due to the following: delayed polar body formation and one failed attempt at first cleavage (Figure 2.11 lower images time stamp 2 h 10 m, 4 h, and 4 h 45 m). This individual still managed to hatch as a swimming blastosquare 1.5 hours later than the next slowest developing individual.

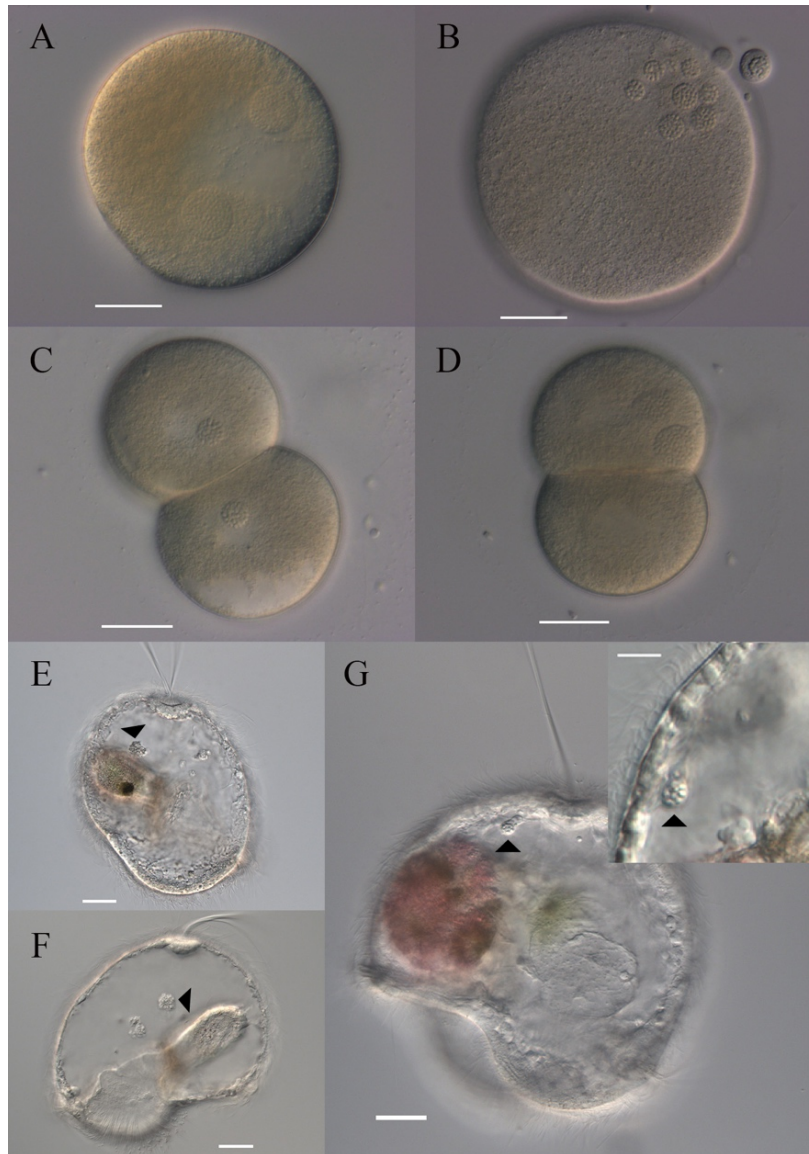
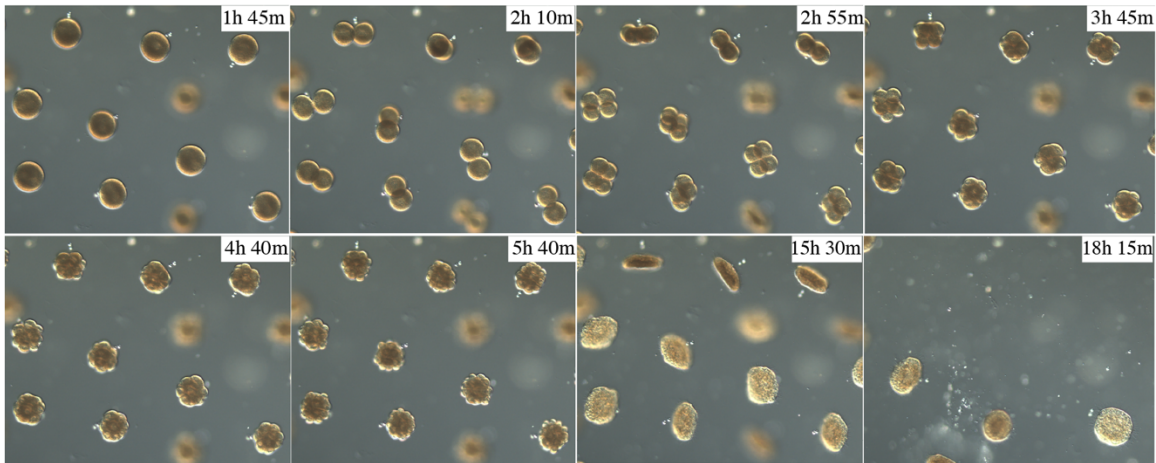


Figure 2.10 – Development of infected oocytes. A – D) Scale bar = 25  $\mu\text{m}$  A) Germinal vesicle breakdown occurring in moderately infected oocyte. B) Infected egg following polar body extrusion with a PSV relocated into a polar body (arrowhead). C, D) Infected embryos following first cleavage. E – F) Scale bar = 50  $\mu\text{m}$ . E) 1-week-old pilidium larva with spore-filled cysts (arrowhead) occupying the larval body cavity. Larva with two apical tufts. F) 2-week-old pilidium larva with spore-filled cysts (arrowhead) in the body cavity. G) 2-week-old pilidium larva with microsporidian spores inside a mesenchyme cell (arrowhead). Scale bar = 50  $\mu\text{m}$ . Inset is the same pilidium at higher magnification. Scale bar = 20  $\mu\text{m}$ .

## Infected



## Uninfected

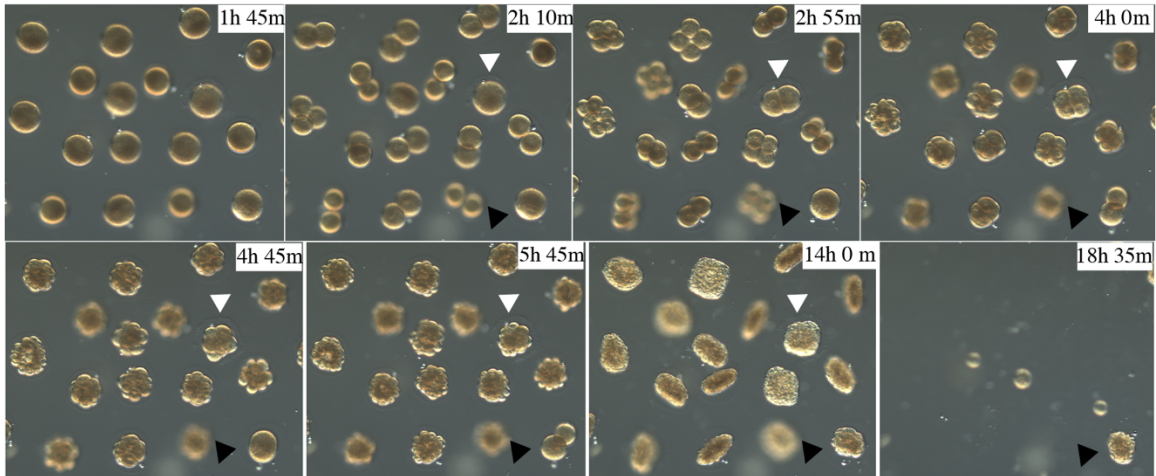


Figure 2.11 – Time lapse video images of *M. alaskensis* development from uninfected oocytes (top images) and infected oocytes (bottom images). Time stamps indicated time post-insemination. Stills in order: before 1<sup>st</sup> cleavage, following 1<sup>st</sup> to 4<sup>th</sup> cleavage of the slowest developing embryo, the 1<sup>st</sup> swimming blastosquare, and final swimming blastosquare. Infected embryo images were taken at the same development points however, the severely delayed embryos (arrowheads) were excluded from the assessment of slowest developing. The slowest developing infected individual (black arrowhead) hatched as a swimming blastosquare at 20 hours and 5 minutes post-insemination.

Oocytes with large areas of cytoplasmic clearing alone, do not test positive for microsporidian infection by PCR indicating these specimens were not carrying any stages of the parasite. Additionally, oocytes only exhibiting a chorion-like investment

surrounding the oocytes did not test positive for infection unless they also contained PSVs with microsporidia inside.

Overtly infected pilidia with obvious and large cysts full of spores were found after one and two weeks of development. One visibly infected 2-week-old pilidium was tested to verify the use of diagnostic PCR on infected larvae. This visible infection, carried inside a mesenchyme cell of the pilidium, was confirmed positive by PCR (Figure 2.10G). To find potential cryptic infections among pilidia larvae, individuals developing from a batch of infected oocytes without visible signs of infection were tested by PCR. Three 1-week old, two 2-week old, six 3-week old, and one 36-day old pilidia were not found to be visibly infected. All visual assessments were confirmed by negative PCR. Further we tested seven newly metamorphosed individuals ranging between 36 and 41-days old. These pilidia were not carrying visible spores prior to metamorphosis and none of the juvenile worms tested positive for microsporidia by PCR.

*Species Description for Hepatosporidae n. gen., n. sp. "Oogranate sp."*

*Description* : Refractile ellipsoid spores are found in large numbers densely packed into PSVs (figure 2.1). Spores measure 2.3 X 1.3  $\mu\text{m}$  ( $2\mu\text{m}^3$ ) in TEM prepared oocytes. The spores are diplokaryotic (Figure 2.2D inset and Figure 2.7A) and contain 6-7 polar tube coils in a single row (figure 2.7A). The spore coat has an electron dense exospore and a thin electron lucent endospore. All life stages are housed within a vesicle capable of interacting with, but separate from the host-cell.

*Diagnosis*: Vesicles containing all life-stages are visible within oocytes of *M. alaskensis* and *M. aquilonia* by light microscopy (Figure 2.4). Spores are also visible by

light microscopy inside mesenchyme cells of developing *M. alaskensis* pilidia (Figure 2.10G). Hoechst and propidium iodide (PPI) staining can be used for detecting diplokarya in cytoplasm of the oocytes even inside whole mount adult tissues. Multiple life-stages are visible in histological sections of ripe female *M. alaskensis*. Spores are also visible by TEM of prepared oocytes. Species specific primers MaMicroF2 and MaMicroR2 can be used for nucleic acid-based diagnosis. Universal microsporidia primers ss18sf and 1492r as well as RPB1-F1 and RPB1-R1 can be used for comparison to full-length sequences pending submission of reference sequences to GenBank (See Table 2.1 for all primer sequences and references).

*Type host:* *M. alaskensis*, *M. aquilonia*, *M. oregonensis*, and *M. cerebrosa*.

*Type locality:* Coos Bay Estuary in Charleston, Oregon.

*Site of infection:* Cytoplasm of *M. alaskensis* and *M. aquilonia* oocytes usually clustering close to the nucleus. Also, the cytoplasm of mesenchyme cells of developing *M. alaskensis* pilidia. Other sites of infection are unknown. Sites of infection within *M. cerebrosa* and *M. oregonensis* are unknown.

*Etymology:* We suggest the name *Oogranate maculaurae*. Genus name for the characteristic spore filled PSVs within oocytes (“oo” oocyte, “granate” many seeds). Species name for the host genus where this organism was originally found. For the purposes of this thesis, this microsporidian is referred to as *Oogranate* sp.

## Discussion

### *Systematics*

Based upon the results of SSU phylogenetics and the protein sequence of RPB1, the novel species *Oogranate* sp. is in the family Hepatosporidae with *Hepatospora*

*eriocheir* as the closest described relative. When comparing morphological features between *Oogranate* sp. and *H. eriocheir*, there are few shared characters (Table 2.2). One of the major differences is in the number of life stages found within a membrane bound vesicle. For *Oogranate* sp. all developmental stages appear to be housed within a parasitophorous vesicle (PSV). In *H. eriocheir*, merogony occurs freely in the cytoplasm while later stages are housed within a vesicle. However, it appears that both species develop by plasmotomy during the merogonial stage. Based on genetics and morphological characters, it is clear these two species are not as closely related as one might expect between members of the same genus so a novel genus has been proposed. It is expected that major taxonomic revisions will follow the discovery of more species in this clade.

Table 2.2 – Comparison of biological and morphological features of microsporidia in the family Hepatosporidae. Type habitat: F - freshwater host. M - marine host.

Microsporidian species	Type host genus	Type habitat	Spores per PSV	Spore size and shape	Polar filament coils	Number of spore nuclei
<i>Hepatospora eriocheir</i>	<i>Eriocheir</i>	Aquatic (F/M)	>60	1.8X0.9µm (ellipsoid)	7-8 (single rank)	unikaryotic
<i>Oogranate</i> sp.	<i>Maculaura</i>	Aquatic (M)	10 <sup>2</sup> – 10 <sup>4</sup>	2.3X1.3µm (ellipsoid)	6-7 (single rank)	diplokaryotic

### Host Types

PCR testing of adult nemertean tissues revealed *Oogranate* sp. DNA within four out of five *Maculaura* species: *M. alaskensis*, *M. aquilonia*, *M. oregonensis*, and *M. cerebrosa*. Infection was visibly observed only in *M. aquilonia* and *M. alaskensis*

oocytes. The only *Maculaura* species where infection was not detected by any technique is *M. magna*, a worm aptly named for its incredibly large body size: the other *Maculaura* average between 3 and 10 cm in length and 1-3 mm in width (depending on the species), whereas specimens of *M. magna* measure on average 20 cm long and 3-4 mm wide (Hiebert & Maslakova, 2015). The size of this nemertean suggests that though it occupies a similar habitat as other *Maculaura* and has the same life history strategy (i.e., a maximally indirect development within a pelagic larva) it may specialize on a different type of prey compared to its smaller relatives. If this microsporidian is trophically transmitted, having a different prey species may protect *M. magna* from infection. The large body size may have enabled escape from this parasite. However, the larger body size may have decreased the chance of finding microsporidian DNA by PCR because a single cross-section of *M. magna* is a lower percent of body coverage when compared to cross-sections of the same volume from a smaller bodied *Maculaura*. Only three *M. magna* from Charleston, Oregon were subjected to testing; more specimens will need to be tested to confirm the absence of *Oogranate* sp. infection in this species.

### *Geographic Distribution*

Microsporidian DNA was detected in adult *M. alaskensis* from Coos Bay and Yaquina Bay, *M. aquilonia* from Coos Bay and Juneau, Alaska, and finally in *M. cerebrosa* and *M. oregonensis* from Coos Bay. Of the 67 susceptible *Maculaura* (excluding *M. magna*) collected from Coos Bay 43.2% tested positive for infection when tested with PCR, a high prevalence for natural parasitic infections. The number of infected worms detected by PCR in Coos Bay stayed between 38-44% over the course of

several sampling months. However, numbers of *M. alaskensis* females bearing visibly infected oocytes seemed to increase in number near the end of the reproductive season (August and September), a trend observed over the last four seasons. The reproductive season of *M. aquilonia* begins and ends earlier in the year than the reproductive season of *M. alaskensis*. The staggering of reproductive seasons leads to several questions: does the intensity of infection increase over the reproductive season and, if so, is this trend observed in all *Maculaura* or just those carrying infection within oocytes (i.e., *M. alaskensis* and *M. aquilonia*)?

Only two infected specimens of *M. alaskensis* were detected within Yaquina Bay in Newport, Oregon (n=17). In Juneau, Alaska, six of 25 *M. aquilonia* sampled in August of 2014 tested positive (24%) of *Maculaura* sampled in August of 2014. These numbers may be underestimations of prevalence considering the potential for false negatives. For example, tissue was collected from the anterior end and posterior end of the same worm and subjected to PCR testing. The posterior end tested positive while the anterior end tested negative. Parasite DNA could be missed during tissue collection or light infections may lead to insufficient recovery of microsporidian DNA during extraction.

Sampling of other host populations is recommended to determine which *Maculaura* are present and susceptible to microsporidian infection in locations outside of Coos Bay. Additionally, all samples for this study were collected within estuary systems. Exploration of infection in *Maculaura* found on the outer shores would be useful for comparing environmental influences, prey availability, or larval retention rates on the intensity and prevalence of infection in this parasite.



### *Parasite Load*

Considering size and numbers of PSVs within infected *M. alaskensis* oocytes, parasite loads for *Oogranate* sp. varied widely. Spore numbers within oocyte PSVs range from  $10^2$  to  $10^4$ . The average oocyte infection recorded from Coos Bay was 2.4 PSVs per oocyte and the median size was 1 picoliter (based on a PSV diameter of 12  $\mu\text{m}$ ). If an *M. alaskensis* oocyte had an approximate of about one quarter of a nanoliter, then a moderate infection of 2.4 PSVs measuring 1 picoliter each might take up only 1% of the oocyte volume but produce  $1.2 \times 10^3$  spores in a single oocyte. The ability of *Oogranate* sp. to produce relatively high spore loads within a single PSV is likely due to infection within oocytes which are one of the largest and best-provisioned cell types.

### *Hypothesized Lifecycle*

By histology in *M. alaskensis*, all the stages we have detected – the proliferative stage (merogony), the spore-forming stage (sporogony), and the infective stage – are separated from contact with oocyte cytoplasm by an interfacial membrane (Figure 2.8). This membrane is likely of host origin since it is found throughout the lifecycle. TEM images show host-cell vesicles docking or leaving the PSV which often indicates a parasitic manipulation of host cellular transport (Weiss & Becnel, 2014).

Figure 2.12 depicts a hypothesized *Oogranate* sp. lifecycle. Infection begins with injection of spore contents into the oocyte cytoplasm. In a single oocyte, we observed a PSV surrounding a light pink staining inclusion. This blister may be the initial formation of the PSV following injection of spore contents into the cell. The meront appears as a dense, uniformly blue stained, circular object within the PSV. The lack of divisions seen

in this object suggests merogony proceeds by plasmotomy, production of a single large cell with many nuclei. Once individual cells are carved from the larger plasmodium they transition to spore formation (Weiss & Becnel, 2014).

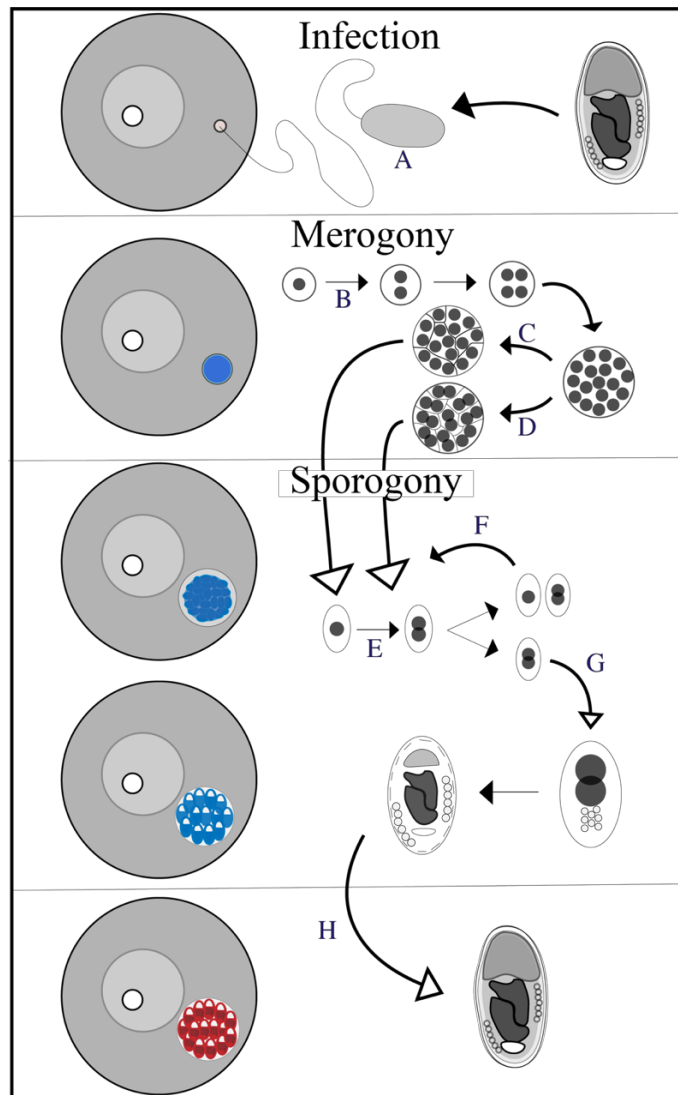


Figure 2.12 – Hypothesized lifecycle of *Oogranate* sp. Oocytes (left) show a histological representation of the lifecycle stage (right). A) Initial infection by injection of spore materials into oocyte cytoplasm and formation of PSV. B) Proliferation proceeds by plasmotomy, where many nuclei are produced inside a single cell body. The plasmodium is carved into individual unikaryon (C) or diplokaryon cells (D) marking the end of merogony. E) Sporogony initiates with division of newly formed cells. The daughter cells will either continue dividing (F) or differentiate (G) by forming specialized spore contents. H) Spore formation is completed by secretion of the spore coat.

During sporogony, as in many other microsporidia, sporonts divide resulting in high spore numbers. It appears the PSV expands outward during this stage, evidenced by a clear ring visible between the developing microsporidia and surrounding envelope, to give room for parasite growth. Cells eventually stop dividing and begin to differentiate, marking the end of sporogony. Individual cells begin to differentiate, developing the polar tube and internally developing the spore surface coat. Sporoblasts appear as individual blue cells with uniform internal structure similar to the configuration observed in completed spores. Spore development concludes with the formation of a completed electron dense coat which stains bright red. This proposed lifecycle requires confirmation by TEM and may proceed differently in other host cells or in the oocytes of other *Maculaura* species.

*M. alaskensis* infections are most apparent and contain heavy parasite loads. However, this finding may be due simply to higher sampling of this species. *M. cerebrosa* is another often-encountered species which tests positive for this microsporidian by PCR. We have not observed overtly infected oocytes in this host, a result which may indicate infection load is lower or present in a different tissue type in this species. A fluorescent in-situ hybridization method or a more thorough histological sampling will be necessary to determine pathology within each host species.

#### *Mode of Transmission in M. alaskensis*

Mode of transmission, whether horizontal or vertical, is a key descriptor of microsporidian species. So far, there is no firm evidence supporting vertical or horizontal transmission of *Oogranate sp.* Using TEM, a single matured spore with extruded polar tube was observed (Figure 2.5). When an infected oocyte is found by histology, several

infected oocytes are found in the same vicinity. This finding could be explained by some fraction of spores auto-maturing within an oocyte, a strategy used by other microsporidian species to pass infection into neighboring cells, resulting in parasite transmission between adjacent oocytes. Across oocyte transmission is a likely mode of *Oogranate* sp. transmission but whether initial infection occurs by ingestion or inheritance is yet to be determined.

### *Vertical Transmission*

There is evidence of infection in gametes and developing larvae, but presence does not guarantee transmission to the juvenile. From this study, it appears infected pilidia do not develop to metamorphosis; however, the pilidia tested came from oocytes of a single *M. alaskensis* female which carried high levels of infection. Only visibly infected pilidia (as detected by light microscopy) up to 2-weeks old tested positive with PCR. Visible infections contained many spores and, therefore, many copies of DNA, while light infections would have fewer copies. A more sensitive reaction, such as a nested or real-time PCR, could be useful for detecting light infections.

Infected pilidia carry spores inside of mesenchyme cells, mobile cells which crawl and transport materials around the larval body. Other microsporidia are known to exploit mobile cell types for migration to specific tissues within the host. For example, in human patients, *Enterocytozoon bieneusi* infects macrophages, a cell similar in structure and function to mesenchyme cells. The parasite could use mesenchyme to enter a developing juvenile rudiment or a tissue likely to be ingested during catastrophic metamorphosis. Using mesenchyme cells could be beneficial or it could be detrimental. As an

immunological cell, the mesenchyme cells may be capable of voiding infection before spores have a chance to infect adjacent cells. With our observation of light infection within an otherwise apparently healthy developing larva (Figure 2.8G), we consider vertical transmission through the pilidium plausible.

#### *Horizontal transmission*

Based on the observation of chaetae within gut contents of dissected *Maculaura*, polychaete worms likely make up part of their natural diet (Maslakova and von Dassow, pers. obs.). *Armandia brevis* is a burrowing polychaete worm found in sandy tidal flats alongside *Maculaura* and is a potential prey for ribbon worms in these environments. In 1970, Szollosi discovered a microsporidian parasite infecting the eggs of *A. brevis* in Friday Harbor, Washington. This microsporidian was classified as *Pleistophora* sp. based on morphological characters (Szollosi, 1970). This species develops within a parasitophorous vesicle, it is diplokaryotic, merogony proceeds by plasmotomy, and it has seven to eight turns of the polar tube in completed spores (Szollosi, 1970). Spore size is not reported; however, based on these other morphological clues, this species may be related to *Oogranate* sp. Other *Pleistophora* sequences found in GenBank are not closely related to the Hepatosporidae but to our knowledge, the *Pleistophora* found infecting eggs of *A. brevis* has not been accounted for in GenBank. If it is closely related, then it may represent another member of the Hepatosporidae; if it is in fact the same species, it may be a source of infection for putative *Armandia* predators such as *Maculaura*.

In horizontal transmission, microsporidia are nearly always found inside the gut epithelia of infected hosts. The nemertean body plan includes gut diverticula which are

closely interwoven with ovaries for nutrient diffusion. This anatomy lends itself to a strategy where spores maturing in the lumen of the gut could puncture through gut and ovarian cell layers to directly infect an oocyte within an adjacent ovary. *Oogranate* sp. infections in *M. alaskensis* seem to cluster around apparent epicenters and are not found in every ovary except in cases of heavy infection. High parasite loads observed in many specimens and the high prevalence found in Coos Bay *Maculaura* may be indicators of horizontal transmission. However, if the parasite is horizontally transmitted, spores should be found within the gut and, so far, there is no evidence of microsporidia anywhere but within oocytes. Given the lack of evidence for successful vertical transmission, *Oogranate* sp. is likely horizontally transmitted in *M. alaskensis* as this is the initial mode of transmission exhibited in microsporidian infections (Weiss & Becnel, 2014).

Infection in other *Maculaura* species may look different than what was observed in *M. alaskensis*. Comparative studies of *Oogranate* sp. infection among the other *Maculaura* species may provide insight into the evolutionary history of these congeners and of their microsporidian parasite which, at present, appears to be walking the line between horizontal and vertical transmission. It may offer clues for how and why this transition takes place and what it means for both host and pathogen.

## CHAPTER 3: CONCLUSION

Aquatic invertebrates make up a significant proportion of animal diversity but studies on parasites of invertebrates have been skewed towards taxa considered to be economically or ecologically important (Morand, Krasnov, & Littlewood, 2015; Poulin & Morand, 2004). Consequently, there is still substantial aquatic parasitic diversity to be explored and documented. For example, some species of nemerteans are regarded as important and ecologically relevant parasites of other organisms (i.e., *Carcinonemertes errans*, an egg parasite of Dungeness crabs) but are rarely considered in the context of their own parasites. To our knowledge there has been no previous documentation of microsporidian parasites infecting the cells or tissues of any members of the phylum Nemertea

With this study, I have shown there is significant need for further research into microsporidian parasites in aquatic invertebrates. A novel microsporidia we call *Oogranate* sp., infects four of five *Maculaura* species tested to varying degrees along the Oregon Coast and in Juneau, Alaska. This microsporidian represents one of only two species within the family Hepatosporidae. Continued research is needed to determine how this parasite may be influencing the biology of host species by comparing infections among these closely related neighboring congeners. Studies of this nature serve not only to broaden our understanding of how microsporidia relate to each other, but serve to create a more thorough understanding of how microsporidia influence their hosts and how these endosymbioses may be driving the evolutionary history of both organisms.

## APPENDIX A

### NEMERTEAN SAMPLE COLLECTION AND EXPERIMENT INFORMATION

Sample Name	Sample Information	Location	Collection	SSU	RPB1	MaMicro	CO1 identity	Histology	TEM	Time lapse
MaPs1	<i>Maculaura</i> oocytes	Portside	7/26/17	no amplification		-				
MaPs2	<i>Maculaura</i> oocytes	Portside	7/26/17	no amplification		-				
MaPs3	<i>Maculaura</i> oocytes	Portside	7/26/17	no amplification		-				
MaPs4	<i>Maculaura</i> oocytes	Portside	7/26/17	no amplification		-				
MaPs5	<i>Maculaura</i> oocytes	Portside	7/26/17	no amplification		-				
MaPs6	<i>Maculaura</i> oocytes	Portside	7/26/17	no amplification		-				
Cere. Pool 1	<i>Cerebratulus</i> sp. n=8	Portside	7/26/17			-				
Paranemertes	<i>Paranemertes</i> sp. n=4	Portside	7/28/17			-				
Cere. Pool 2	<i>Cerebratulus</i> sp. n=8	Fisherman's Grotto	8/3/17			-				
MaPsIn 17-1	<i>Maculaura</i> oocytes	Portside	8/25/17	yes amplification	yes amplification	+				
MaPsIn 17-2	<i>Maculaura</i> oocytes	Portside	9/4/17	no amplification	no amplification	-		yes		
MaPsIn 17-3	<i>Maculaura</i> oocytes	Portside	9/4/17	yes amplification	no amplification	+		yes		
MaPsIn 17-4	<i>Maculaura</i> oocytes	Portside	9/4/17	yes amplification	no amplification	+		yes		
MaPsIn 17-5	<i>Maculaura</i> oocytes	Portside	9/4/17	yes amplification	no amplification	+		yes		
Green Pool 1	<i>Emplectonema</i> sp. n=4	Metcalf Marsh	8/6/17			-				
Cere. Pool 3	<i>Cerebratulus</i> sp. n=4	Portside	1/30/18			-				
MaPsIn 18.1	<i>Maculaura</i> oocytes	Portside	1/30/18	yes amplification	yes amplification	+				
Maculaura 1	adult	Portside	1/30/18			-				
Maculaura 2	adult	Portside	1/30/18			-				



Sample Name	Sample Information	Location	Collection	SSU	RPB1	MaMicro	CO1 identity	Histology	TEM	Time lapse
Maculaura 3	adult	Portside	1/30/18			+	<i>Maculaura aquilonia</i>			
Maculaura 4	adult	Portside	1/30/18			-				
Maculaura 5	adult	Portside	1/30/18			-				
Maculaura 6	adult	Portside	1/30/18			-				
Maculaura 7	adult	Portside	1/30/18			-				
Maculaura 8	adult	Portside	1/30/18			-				
Maculaura 9	adult	Portside	1/30/18			+	<i>Maculaura alaskensis</i>			
Maculaura 10	adult	Portside	1/30/18			+	<i>Maculaura alaskensis</i>			
Maculaura 11	adult	Portside	1/30/18			-				
Maculaura 12	adult	Portside	1/30/18			-				
Maculaura 13	adult	Portside	3/9/18			-				
Maculaura 14	adult	Portside	3/9/18			-				
Maculaura 15	adult	Portside	3/9/18			-				
Maculaura 16	adult	Portside	3/9/18			+	<i>Maculaura alaskensis</i>			
Maculaura 17	adult	Portside	3/9/18			-				
Maculaura 18	adult	Portside	3/9/18			+	<i>Maculaura aquilonia</i>			
Maculaura 19	adult	Portside	3/9/18			+	<i>Maculaura alaskensis</i>			
Maculaura 20	adult	Portside	3/9/18			-				
Maculaura 21	adult	Portside	3/9/18			+	<i>Maculaura alaskensis</i>			
Maculaura 22	adult	Portside	3/9/18			+	<i>Maculaura cerebrosa</i>			
Maculaura 23	adult	Portside	3/9/18			-				
Maculaura 25	adult	Portside	3/9/18			-				
Maculaura 26	adult	Portside	3/9/18			-				
Maculaura 27	adult	Portside	3/9/18			+	<i>Maculaura alaskensis</i>			
Maculaura 28	adult	Portside	3/9/18			-				
Maculaura 29	adult	Portside	3/9/18			+	<i>Maculaura cerebrosa</i>			

Sample Name	Sample Information	Location	Collection	SSU	RPB1	MaMicro	CO1 identity	Histology	TEM	Time lapse
Maculaura 30	adult	Portside	3/9/18			-				
Maculaura 31	adult	Metcalf Marsh	3/27/18			-				
Maculaura 32	adult	Metcalf Marsh	3/27/18			-				
Maculaura 33	adult	Metcalf Marsh	3/27/18			+	<i>Maculaura alaskensis</i>			
Maculaura 34	adult	Metcalf Marsh	3/27/18			-				
Maculaura 35	adult	Metcalf Marsh	3/27/18			+	<i>Maculaura alaskensis</i>			
Maculaura 36	adult	Metcalf Marsh	3/27/18			-				
Maculaura 37	adult	Metcalf Marsh	3/27/18			+	<i>Maculaura alaskensis</i>			
Maculaura 38	adult	Metcalf Marsh	3/27/18			+	<i>Maculaura alaskensis</i>			
Maculaura 39	adult	Metcalf Marsh	3/27/18			+	<i>Maculaura alaskensis</i>			
Maculaura 40	adult	Metcalf Marsh	3/27/18			-				
Maculaura 41	adult	Metcalf Marsh	3/27/18			+	<i>Maculaura alaskensis</i>		yes	
Maculaura 42	adult	Portside Rocks	4/9/18			+	<i>Maculaura alaskensis</i>		yes	
Maculaura 43	adult	Portside Rocks	4/9/18			+	<i>Maculaura alaskensis</i>			
Maculaura 44	adult	Portside Rocks	4/9/18			-				
Maculaura 45	adult	Portside Rocks	4/9/18			-				
Maculaura 46	adult	Portside Rocks	4/9/18			-				
Maculaura 47	adult	Portside Rocks	4/9/18			-				
Maculaura 48	adult	Portside Rocks	4/9/18			-				
Maculaura 49	adult	Portside Rocks	4/9/18			+	<i>Maculaura alaskensis</i>			
Maculaura 50	adult	Hatfield Marsh	5/13/18			-				
Maculaura 51	adult	Hatfield Marsh	5/13/18			-				
Maculaura 52	adult	Hatfield Marsh	5/13/18			-				
Maculaura 53	adult	Hatfield Marsh	5/13/18			-				
Maculaura 54	adult	Hatfield Marsh	5/13/18			+	<i>Maculaura alaskensis</i>			
Maculaura 55	adult	Hatfield Marsh	5/13/18			-				

Sample Name	Sample Information	Location	Collection	SSU	RPB1	MaMicro	CO1 identity	Histology	TEM	Time lapse
Carinoma Pool	<i>Carinoma sp.</i> n=3	Hatfield Marsh	5/13/18			-				
Cere Pool 4	<i>Cerebratulus sp.</i> n=4	Hatfield Marsh	5/13/18			-				
Maculaura 56	adult	Fisherman's Grotto	5/30/18			-				
Maculaura 57	adult	Fisherman's Grotto	5/30/18			-				
Maculaura 58	adult	Fisherman's Grotto	5/30/18			+	<i>Maculaura alaskensis</i>			
Maculaura 59	adult	Fisherman's Grotto	5/30/18			+	<i>Maculaura alaskensis</i>			
Maculaura 60	adult	Fisherman's Grotto	5/30/18			+	<i>Maculaura oregonensis</i>			
Maculaura 61	adult	Fisherman's Grotto	5/30/18			-				
Maculaura 62	adult	Fisherman's Grotto	5/30/18			+	<i>Maculaura aquilonia</i>			
Maculaura 63	adult	Fisherman's Grotto	5/30/18			-				
Maculaura 64	adult	Fisherman's Grotto	5/30/18			+				
Maculaura 65	adult	Fisherman's Grotto	5/30/18			+	<i>Maculaura alaskensis</i>			
Maculaura 66	adult	Fisherman's Grotto	5/30/18			-				
Maculaura 67	adult	Fisherman's Grotto	5/30/18			+	<i>Maculaura alaskensis</i>			
Maculaura 68	adult	Fisherman's Grotto	5/30/18			+	<i>Maculaura alaskensis</i>			
Maculaura 69	adult	Portside	5/30/18			-				
Maculaura 70	adult	Portside	5/30/18			-				
<i>Maculaura magna</i>	adult	Portside	5/30/18			-				
Lineus pool	<i>Lineus sp.</i> red n=3	Portside	5/30/18			-				
Mac 71	adult	Portside	5/30/18			-				
Mac 72	adult	Portside	5/30/18			-				
Mac 73	adult	Portside	5/30/18			+	<i>Maculaura oregonensis</i>			
Mac 74	adult	Portside	9/2/18			-				

Sample Name	Sample Information	Location	Collection	SSU	RPB1	MaMicro	CO1 identity	Histology	TEM	Time lapse
Mac 75	adult	Portside	9/2/18			-				
Mac 76	adult	Hatfield Marsh	9/11/18			-				
Mac 77	adult	Hatfield Marsh	9/11/18			-				
Mac 78	adult	Hatfield Marsh	9/11/18			-				
Mac 79	adult	Hatfield Marsh	9/11/18			-				
Mac 80	adult	Hatfield Marsh	9/11/18			+	<i>Maculaura alaskensis</i>			
Mac 81	adult	Hatfield Marsh	9/11/18			-				
Mac 82	adult	Hatfield Marsh	9/11/18			-				
Mac 83	adult	Hatfield Marsh	9/11/18			-				
Mac 84	adult	Hatfield Marsh	9/11/18			-				
Mac 85	adult	Hatfield Marsh	9/11/18			-				
Mac 86	adult	Hatfield Marsh	9/11/18			-				
Video 1	adult	Portside	9/1/18							yes
Video 2	adult	Portside	9/1/18							yes
Video 3	adult	Portside	9/1/18			+	<i>Maculaura alaskensis</i>			yes
Pil 2	1 week		9/14/28			-				
Pil 3	1 week		9/14/28			-				
Pil 4	1 week		9/14/28			-				
Pil 6	2 weeks		9/21/18			-				
Pil 11	2 weeks		9/21/18			+	<i>Maculaura alaskensis</i>			
Pil 12	3 weeks		9/28/18			-				
Pil 13	3 weeks		9/28/18			-				
Pil 14	3 weeks		9/28/18			-				
Pil 15	3 weeks		9/28/18			-				
Pil 16	3 weeks		9/28/18			-				
Pil 17	3 weeks		9/28/18			-				
Pil 19	30 days		10/7/18			-				
Pil 20	30 days		10/7/18			-				

Sample Name	Sample Information	Location	Collection	SSU	RPB1	MaMicro	CO1 identity	Histology	TEM	Time lapse
Pil 21	30 days		10/7/18			-				
Pil 30	36 days		10/13/18			-				
M1	36 d - metamorphosis		10/13/18			-				
M2	40 d - metamorphosis		10/17/18			-				
M3	40 d - metamorphosis		10/17/18			-				
M4	40 d - metamorphosis		10/17/18			-				
M5	41 d - metamorphosis		10/18/18			-				
M6	41 d - metamorphosis		10/18/18			-				
Pil MX	41 d incomplete metamorphosis		10/18/18			-				
J5-08VII		Lena Beach	8/8/14			-				
J10-09VII		Auke Bay	8/9/14			-				
J11-09VII		Auke Bay	8/9/14			-				
J12-08VII		Auke Bay	8/9/14			+	<i>Maculaura aquilonia</i>			
J15		Auke Creek	8/10/14			-				
J16		Auke Creek	8/10/14			-				
J17		Auke Creek	8/10/14			+	<i>Maculaura aquilonia</i>			
J18		Auke Creek	8/10/14			+	<i>Maculaura aquilonia</i>			
J19		Auke Creek	8/10/14			-				
J20		Auke Creek	8/10/14			-				
J21		Auke Creek	8/10/14			-				
J22		Auke Creek	8/10/14			-				
J23		Auke Creek	8/10/14			-				
J36		Bridget Cove	8/11/14			-				
J45		Sheep Creek	8/12/14			+	<i>Maculaura aquilonia</i>			
J46		Sheep Creek	8/12/14			-				
J47		Sheep Creek	8/12/14			-				

Sample Name	Sample Information	Location	Collection	SSU	RPB1	MaMicro	CO1 identity	Histology	TEM	Time lapse
J48		Outer Point	8/13/14			-				
J49		Outer Point	8/13/14			+	<i>Maculaura aquilonia</i>			
J50		Outer Point	8/13/14			-				
J51		Outer Point	8/13/14			-				
J52		Outer Point	8/13/14			-				
J53		Outer Point	8/13/14			-				
J54		Outer Point	8/13/14			-				
J55		Outer Point	8/13/14			-				
J56		Outer Point	8/13/14			-				
J57		Outer Point	8/13/14			-				
J58		Outer Point	8/13/14			-				
J59		Outer Point	8/13/14			+	<i>Maculaura aquilonia</i>			
J60		Outer Point	8/13/14			-				

## APPENDIX B

### NCBI SEQUENCES AND ACCESSION NUMBERS

Accession Number	Species Name	Accession Number	Species Name
KF549987	<i>Agmasoma penaei</i>	AJ438961	<i>Dictyocoela deshayesum</i>
AY090068	<i>Amblyospora bracteata</i>	AF397404	<i>Dictyocoela duebenum</i>
U68473	<i>Amblyospora californica</i>	AJ438958	<i>Dictyocoela gammarellum</i>
AY090056	<i>Amblyospora canadensis</i>	AJ438956	<i>Dictyocoela muelleri</i>
AY090057	<i>Amblyospora cinerei</i>	AF027684	<i>Edhazardia aedis</i>
AF025685	<i>Amblyospora connecticus</i>	L39107	<i>Encephalitozoon cuniculi</i>
AY090061	<i>Amblyospora criniferis</i>	L39108	<i>Encephalitozoon hellem</i>
AY090043	<i>Amblyospora excrucii</i>	AF067144	<i>Encephalitozoon lacertae</i>
AY090062	<i>Amblyospora ferocious</i>	KR998311	<i>Encephalitozoon pogonae</i>
AY090045	<i>Amblyospora khaliulini</i>	AY009115	<i>Endoreticulatus bombycis</i>
AY090052	<i>Amblyospora opacita</i>	L39109	<i>Endoreticulatus schubergi</i>
AY090049	<i>Amblyospora stictici</i>	JX915760	<i>Enterocytophora artemiae</i>
AF027685	<i>Amblyospora stimuli</i>	L07123	<i>Enterocytozoon bienensei</i>
AY090048	<i>Amblyospora weiseri</i>	KY643648	<i>Enterocytozoon hepatopenaei</i>
KJ652549	<i>Ameson metacarcini</i>	AF201911	Enterocytozoonidae gen. sp.
L15741	<i>Ameson michaelis</i>	HE584634	<i>Enterospora canceri</i>
KC915038	<i>Ameson portunus</i>	KT762153	<i>Globulispora mitoportans</i>
KX214674	<i>Amphiamblys</i> sp.	AF056014	<i>Glugea americanus</i>
AY894423	<i>Anncaliia meligethi</i>	AF044391	<i>Glugea anomala</i>
AF024655	<i>Antonospora scoticae</i>	U15987	<i>Glugea atherinae</i>
AJ581995	<i>Bacillidium vesiculoformis</i>	AF394525	<i>Glugoides intestinalis</i>
AY090042	<i>Berwaldia schaefernai</i>	AF439320	<i>Gurleya daphniae</i>
AF484690	<i>Bryonosema plumatellae</i>	AF394526	<i>Gurleya vavrai</i>
AF132544	<i>Caudospora palustris</i>	AJ302318	<i>Hamiltosporidium magnivora</i>
AY090054	<i>Culicospora magna</i>	HE584635	<i>Hepatospora eriocheir</i>
AF027683	<i>Culicosporella lunata</i>	AB623036	<i>Heterosporis anguillarum</i>
AY233131	<i>Cystosporogenes legeri</i>	HE584635	<i>Hepatospora eriocheir</i>
AJ302320	<i>Cystosporogenes operophterae</i>	AB623036	<i>Heterosporis anguillarum</i>
AJ438957	<i>Dictyocoela berillonum</i>	AF356225	<i>Heterosporis</i> sp.
AJ438960	<i>Dictyocoela cavimanum</i>	AF483837	<i>Hyalinocysta chapmani</i>

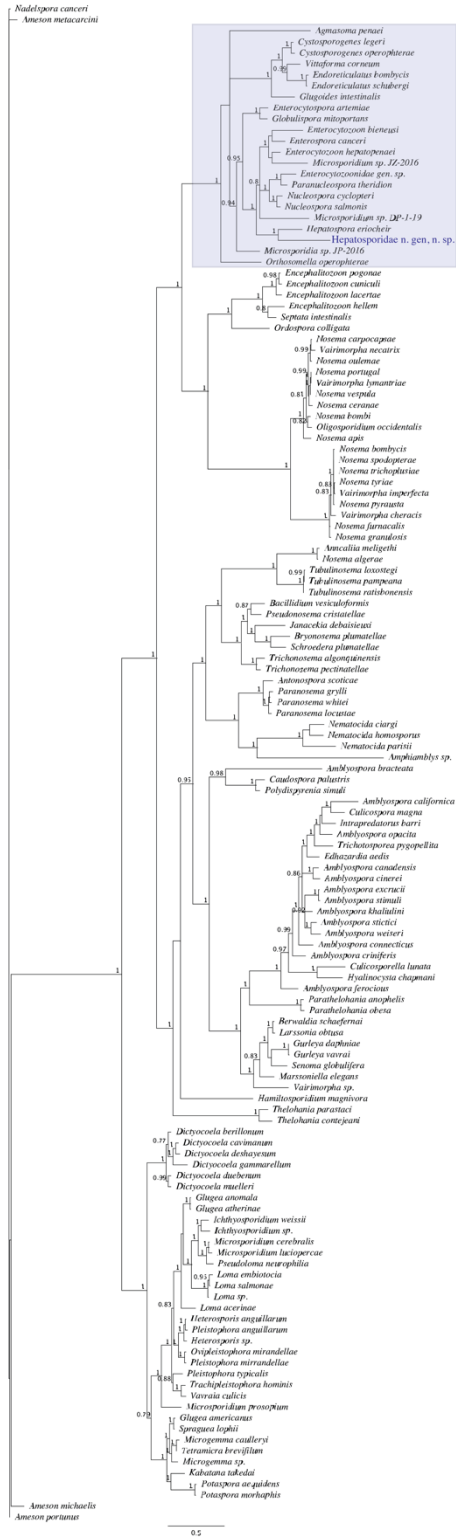
Accession Number	Species Name	Accession Number	Species Name
L39110.1	<i>Ichthyosporidium</i> sp.	AY211392	<i>Nosema spodopterae</i>
JQ062988	<i>Ichthyosporidium weissii</i>	U09282	<i>Nosema tricholplusiae</i>
AY013359	<i>Intrapredatorus barri</i>	AJ012606	<i>Nosema tyriae</i>
AY090070	<i>Janacekia debaisieuxi</i>	U11047	<i>Nosema vespula</i>
AF356222	<i>Kabatana takedai</i>	KC203457	<i>Nucleospora cyclopteri</i>
AF394527	<i>Larssonia obtusa</i>	U78176	<i>Nucleospora salmonis</i>
AJ252951	<i>Loma acerinae</i>	AF495379	<i>Oligosporidium occidentalis</i>
AF320310	<i>Loma embiotocia</i>	AF394529	<i>Ordospora colligata</i>
U78736	<i>Loma salmonae</i>	AJ302317	<i>Orthosomella operophtherae</i>
AF104081	<i>Loma</i> sp.	AF356223	<i>Ovipleistophora mirandellae</i>
AY090041	<i>Marssoniella elegans</i>	AY305325	<i>Paranosema grylli</i>
AY033054	<i>Microgemma caulleryi</i>	AY305324	<i>Paranosema locustae</i>
AJ252952	<i>Microgemma</i> sp.	AY305323	<i>Paranosema whitei</i>
JQ316511	<i>Microsporidium cerebralis</i>	KR187184	<i>Paranucleospora theridion</i>
KX351969	<i>Micropsoridium luciopercae</i>	AF027682	<i>Parathelohania anophelis</i>
AF151529	<i>Microsporidium prosopium</i>	AY090065	<i>Parathelohania obesa</i>
AF394528	<i>Microsporidium</i> sp. DP-1-19	AF044387	<i>Pleistophora typicalis</i>
KR263870	<i>Microsporidium</i> sp. JZ-2016	U47052	<i>Pleistophora anguillarum</i>
FJ794873	<i>Microsporidium</i> sp. MIC2	AF104085	<i>Pleistophora mirrandellae</i>
AY958070	<i>Nadelspora canceri</i>	AY090069	<i>Polydispyrenia simuli</i>
KX360152	<i>Nematocida ciargi</i>	KP404613	<i>Potaspora aequidens</i>
KX360153	<i>Nematocida homosporus</i>	EU534408	<i>Potaspora morhaphis</i>
XR_001214623	<i>Nematocida parisii</i>	AF322654	<i>Pseudoloma neurophilia</i>
AF0690963	<i>Nosema algerae</i>	AF484694	<i>Pseudonosema cristatellae</i>
X73894	<i>Nosema apis</i>	AY135024	<i>Schroedera plumatellae</i>
AY008373	<i>Nosema bombi</i>	AF484695	<i>Trichonosema pectinatellae</i>
L39111	<i>Nosema bombycis</i>	HM594267	<i>Trichotosporea pygopellita</i>
AF426104	<i>Nosema carpocapsae</i>	JQ906779	<i>Tubulinosema loxostegi</i>
U26533	<i>Nosema ceranae</i>	KM883008	<i>Tubulinosema pampeana</i>
U26552	<i>Nosema furnacalis</i>	AY695845	<i>Tubulinosema ratisbonensis</i>
AJ011833	<i>Nosema granulosis</i>	DQ641245	<i>Senoma globulifera</i>
U27359	<i>Nosema oulemae</i>	L39113	<i>Septata intestinalis</i>
AF033316	<i>Nosema portugal</i>	AF033197	<i>Spraguea lophii</i>
AY958071	<i>Nosema pyrausta</i>	AF364303	<i>Tetramicra brevifilum</i>



Accession Number	Species Name	Accession Number	Species Name
AF492593	<i>Thelohania contejeani</i>	AF033315	<i>Vairimorpha lymantriae</i>
AF294779	<i>Thelohania parastaci</i>	Y00266	<i>Vairimorpha necatrix</i>
AJ002605	<i>Trachipleistophora hominis</i>	AF031539	<i>Vairimorpha sp.</i>
AY582742	<i>Trichonosema algonquinensis</i>	AJ252961	<i>Vavraia culicis</i>
AF327408	<i>Vairimorpha cheracis</i>	L39112	<i>Vittaforma corneum</i>
AJ131645	<i>Vairimorpha imperfecta</i>		

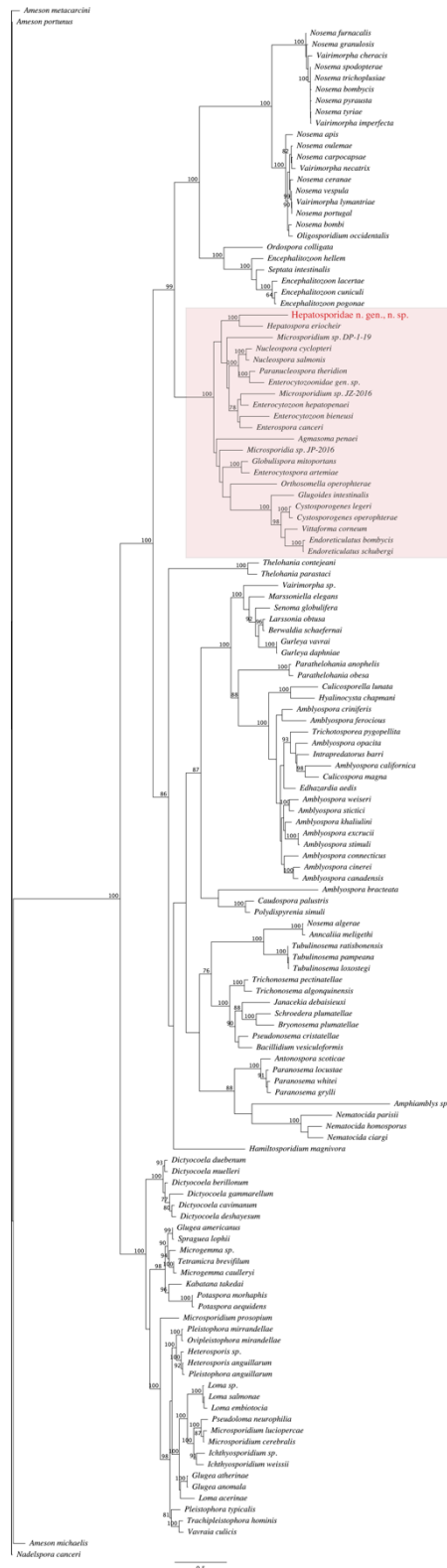
# APPENDIX C

## COMPLETE BAYESIAN INFERENCE PHYLOGENETIC TREE



# APPENDIX D

## COMPLETE MAXIMUM-LIKELIHOOD PHYLOGENETIC TREE



## APPENDIX E

### EPIDEMIOLOGY DATA FOR INFECTED OOCYTES COLLECTED IN 2017

ID	Collection Location	Date	Number Infected	Number of Uninfected	% Infected	PSV Count	Average PSV Count	Max PSV Count
MaPsIn 17-1	Portside	8/25/17	32	170	0.158	91	2.844	10
MaPsIn 17-2	Portside	8/25/17	32	222	0.126	82	2.5625	12
MaPsIn 17-3	Portside	8/25/17	10	182	0.052	18	1.8	8
MaPsIn 17-5	Portside	8/25/17	13	88	0.129	29	2.2308	8

## REFERENCES CITED

- Ardila-Garcia, A. M., & Fast, N. M. (2012). Microsporidian infection in a free-living marine nematode. *Eukaryotic Cell*, *11*(12), 1544–1551. doi: 10.1128/EC.00228-12
- Bandi, C., Dunn, A. M., Hurst, G. D. D., & Rigaud, T. (2001). Inherited microorganisms, sex-specific virulence and reproductive parasitism. *Trends in Parasitology*, *17*(2), 88–94. doi: 10.1016/S1471-4922(00)01812-2
- Bird, A. M., von Dassow, G., & Maslakova, S. A. (2014). How the pilidium larva grows. *EvoDevo*, *5*, 13. doi: 10.1186/2041-9139-5-13
- Bojko, J., Clark, F., Bass, D., Dunn, A. M., Stewart-Clark, S., Stebbing, P. D., & Stentiford, G. D. (2017). *Parahepatospora carcini* n. gen., n. sp., a parasite of invasive *Carcinus maenas* with intermediate features of sporogony between the Enterocytozoon clade and other microsporidia. *Journal of Invertebrate Pathology*, *143*, 124–134. <https://doi.org/https://doi.org/10.1016/j.jip.2016.12.006>
- Coe, W. R. (1905). *Nemerteans of the west and northwest coasts of America* (Bulletin of the Museum of Comparative Zoology at Harvard College, Vol. 47). Cambridge, MA: Printed for the Museum.
- Corradi, N., & Keeling, P. J. (2009). Microsporidia: A journey through radical taxonomical revisions. *Fungal Biology Reviews*, *23*(1–2), 1–8. doi: 10.1016/j.fbr.2009.05.001
- Corradi, N. (2015). Microsporidia: Eukaryotic intracellular parasites shaped by gene loss and horizontal gene transfers. *Annual Review of Microbiology*, *69*(1), 167–183. doi: 10.1146/annurev-micro-091014-104136
- Dunn, A. M., & Smith, J. E. (2001). Microsporidian life cycles and diversity: The relationship between virulence and transmission. *Microbes and Infection*, *3*(5), 381–388. doi: 10.1016/S1286-4579(01)01394-6
- Folmer, O., Black, M., Hoeh, W., Lutz, R., & Vrijenhoek, R. (1994). DNA primers for amplification of mitochondrial cytochrome *c* oxidase subunit I from diverse metazoan invertebrates. *Molecular Marine Biology and Biotechnology*, *3*(5), 294–299. doi: 10.1371/journal.pone.0013102
- Franzen, C. (2008). Microsporidia: A review of 150 years of research. *The Open Parasitology Journal*, *2*, 1–34. doi: 10.2174/1874421400802010001

- Hiebert, T. C., & Maslakova, S. (2015). Integrative Taxonomy of the *Micrura alaskensis* Coe, 1901 Species Complex (Nemertea: Heteronemertea), with Descriptions of a New Genus *Maculaura* gen. nov. and Four New Species from the NE Pacific. *Zoological Science*, 32(6), 615–37. <https://doi.org/10.2108/zs150011>
- Hirt, R. P., Logsdon, J. M., Healy, B., Dorey, M. W., Doolittle, W. F., & Embley, T. M. (1999). Microsporidia are related to Fungi: evidence from the largest subunit of RNA polymerase II and other proteins. *Proceedings of the National Academy of Sciences*, 96(2), 580-585.
- Ironside, J. E., Smith, J. E., Hatcher, M. J., Sharpe, R. G., Rollinson, D., & Dunn, A. M. (2003). Two species of feminizing microsporidian parasite coexist in populations of *Gammarus duebeni*. *Journal of Evolutionary Biology*, 16(3), 467–473.
- Keeling, P. J., & Fast, N. M. (2002). Microsporidia: Biology and evolution of highly reduced intracellular parasites. *Annual Review of Microbiology*, 56(1), 93–116. doi: 10.1146/annurev.micro.56.012302.160854
- Lom, J., & Vavra, J. (1963). The mode of sporoplasm extrusion in microsporidian spores. *Acta Protozoologica*, 1(1-13), 81-90.
- Maslakova, S. a. (2010). Development to metamorphosis of the nemertean pilidium larva. *Frontiers in Zoology*, 7(1), 30. <https://doi.org/10.1186/1742-9994-7-30>
- McDermott, J. J. (2006). Nemerteans as hosts for symbionts: A review. *Journal of Natural History*, 40(15–16), 1007–1020. doi: 10.1080/00222930600834121
- Morand, S., Krasnov, B. R., & Littlewood, D. T. J. (2015). *Parasite diversity and diversification*. Cambridge University Press.
- Poulin, R., & Morand, S. (2014). *Parasite biodiversity*. Washington D.C.: Smithsonian Institution.
- Reynolds, E. S. (1963). The use of lead citrate at high pH as an electron-opaque stain in electron microscopy. *The Journal of Cell Biology*, 17(1), 208.
- Ryan, J. A., & Kohler, S. L. (2010). Virulence is context-dependent in a vertically transmitted aquatic host–microparasite system. *International Journal for Parasitology*, 40(14), 1665–1673. doi: 10.1016/j.ijpara.2010.07.004
- Stentiford, G. D., Bateman, K. S., Dubuffet, A., Chambers, E., & Stone, D. M. (2011). *Hepatospora eriocheir* (Wang and Chen, 2007) gen. et comb. nov. infecting invasive Chinese mitten crabs (*Eriocheir sinensis*) in Europe. *Journal of Invertebrate Pathology*, 108(3), 156–166.

- Stentiford, G. D., Feist, S. W., Stone, D. M., Bateman, K. S., & Dunn, A. M. (2013). Microsporidia: Diverse, dynamic, and emergent pathogens in aquatic systems. *Trends in Parasitology*, 29(11), 567–578. doi: 10.1016/j.pt.2013.08.005
- Stricker, S. A. (1992). Phylum Nemertea. In M. F. Strathman (Ed.), *Reproduction and development of marine invertebrates of the northern Pacific coast: data and methods for the study of eggs, embryos, and larvae* (pp. 129-137). Seattle, Washington: University of Washington Press.
- Szollosi, D. (1971). Development of *Pleistophora* sp.(Microsporidian) in eggs of the polychaete *Armandia brevis*. *Journal of invertebrate pathology*, 18(1), 1-15.
- Vinckier, D. (1975). *Nosemoides* gen. n., *N. vivieri* (Vinckier, Devauchelle, & Prensier, 1970) comb. nov. (Microsporidie); Etude de la différenciation sporoblastique et genèse des différentes structures de la spore. *The Journal of Protozoology*, 22(22), 170–184. doi: 10.1111/j.1550-7408.1975.tb05846.x
- Vinckier, D., Devauchelle, G., & Prensier, G. (1970). *Nosema vivieri* n. sp.(Microsporidae, Nosematidae) hyperparasite of gregarina living in nemertina coelom. *Comptes Rendus Hebdomadaires Des Seances de l'Academie Des Sciences. Serie D: Sciences Naturelles*, 270(6), 821-823.
- von Dassow, G., & Maslakova, S. A. (2017). The trochoblasts in the pilidium larva break an ancient spiralian constraint to enable continuous larval growth and maximally indirect development. *EvoDevo*, 8(1), 19.
- Vossbrinck, C. R., & Debrunner-Vossbrinck, B. A. (2005). Molecular phylogeny of the Microsporidia: ecological, ultrastructural and taxonomic considerations. *Folia Parasitologica*, 52(1/2), 131.
- Wang, W., & Chen, J. (2007). Ultrastructural study on a novel microsporidian, *Endoreticulatus eriocheir* sp. nov.(Microsporidia, Encephalitozoonidae), parasite of Chinese mitten crab, *Eriocheir sinensis* (Crustacea, Decapoda). *Journal of Invertebrate Pathology*, 94(2).
- Weber, R., Bryan, R. T., Owen, R. L., Wilcox, C. M., Gorelkin, L., Visvesvara, G. S., & the Enteric Opportunistic Infections Working Group. (1992). Improved light-microscopical detection of microsporidia spores in stool and duodenal aspirates. *New England Journal of Medicine*, 326(3), 161–166. doi: 10.1056/NEJM199201163260304
- Weiss, L. M., Edlind, T. D., Vossbrinck, C. R., & Hashimoto, T. (1999). Microsporidian molecular phylogeny: The fungal connection. *The Journal of Eukaryotic Microbiology*, 46(5), 17S-18S. doi: 10.1111/j.1550-7408.1999.tb06055.x

Weiss, L. M., & Becnel, J. J. (Eds.). (2014). *Microsporidia: Pathogens of opportunity*. Ames, IA: Wiley Blackwell.

Weiss, L. M., & Vossbrinck, C. R. (1999). Molecular biology, molecular phylogeny, and molecular diagnostic approaches to the microsporidia. In *The microsporidia and microsporidiosis* (pp. 129-171). American Society of Microbiology.

Wittner, M., & Weiss, L. M. (Eds.). (1999). *The microsporidia and microsporidiosis*. Washington DC: ASM press.